bioRxiv preprint doi: https://doi.org/10.1101/2020.10.29.360487; this version posted October 29, 2020. The copyright holder for this preprint (which was not certified by peer review) is the author/funder, who has granted bioRxiv a license to display the preprint in perpetuity. It is made available under aCC-BY-NC-ND 4.0 International license.

# Low nitrogen availability inhibits the phosphorus starvation response in maize (*Zea mays* ssp. *mays* L.)

J. Vladimir Torres-Rodríguez[1], M. Nancy Salazar-Vidal[1,2,3], Ricardo A. Chávez Montes[1,4], Julio A. Massange-Sánchez[5], C. Stewart Gillmor[1], Ruairidh J. H. Sawers[1,6*]

[1] Laboratorio Nacional de Genómica para la Biodiversidad (Langebio), Unidad de Genómica Avanzada, Centro de Investigación y de Estudios Avanzados del Instituto Politécnico Nacional (CINVESTAV-IPN), Irapuato, C.P. 36824, Guanajuato, México.

[2] Department of Evolution and Ecology, University of California–Davis, One Shields Avenue, Davis, CA 95616, USA.

[3] Division of Plant Sciences, Univ. of Missouri, Columbia, MO 65211, USA

[4] Institute of Genomics for Crop Abiotic Stress Tolerance, Texas Tech University, Lubbock, TX, 79409, USA.

[5] Unidad de Biotecnología Vegetal, Centro de Investigación y Asistencia en Tecnología y Diseño del Estado de Jalisco A.C. (CIATEJ) Subsede Zapopan, Guadalajara, México.

[6] Department of Plant Science, The Pennsylvania State University, State College, PA, USA.

* Author for correspondence: ruairidh.sawers@gmail.com

bioRxiv preprint doi: https://doi.org/10.1101/2020.10.29.360487; this version posted October 29, 2020. The copyright holder for this preprint (which was not certified by peer review) is the author/funder, who has granted bioRxiv a license to display the preprint in perpetuity. It is made available under aCC-BY-NC-ND 4.0 International license.

## ABSTRACT

### Background

Nitrogen (N) and phosphorus (P) are macronutrients essential for crop growth and productivity. In cultivated fields, N and P levels are rarely sufficient, contributing to the yield gap between realized and potential production. Fertilizer application increases nutrient availability, but not all farmers have access to such additions, nor are current rates of application sustainable or environmentally desirable. Transcriptomic studies of cereal crops have revealed dramatic responses to either low N or low P single stress treatments. In the field, however, levels of both N and P may be suboptimal. The interaction between N and P starvation responses remains to be fully characterized.

### Results

We characterized the root and leaf transcriptomes of young maize plants grown under control, low N, low P or combined low NP conditions. We identified 1, 555 genes that responded to at least one of the treatments, in at least one of the tissues. Transcriptional responses to low N and low P were distinct, with very few genes responding in a similar way to the two single stress treatments. Furthermore, the regulation of a large group of genes was antagonistic between the two conditions. In combined NP stress, the low N response dominated, the classical P starvation response being largely suppressed. An additional experiment over a range of N availability indicated that even a mild reduction in N levels was sufficient to repress the low P induction of well-characterized P starvation genes. Although expression of P transporter genes was repressed under low N or low NP, we confirmed earlier reports of P hyper accumulation under low N. To lay the foundations for further study of the mechanistic basis of NP signaling in maize, we

bioRxiv preprint doi: https://doi.org/10.1101/2020.10.29.360487; this version posted October 29, 2020. The copyright holder for this preprint (which was not certified by peer review) is the author/funder, who has granted bioRxiv a license to display the preprint in perpetuity. It is made available under aCC-BY-NC-ND 4.0 International license.

annotated the complete set of maize *Spx* genes, and found evidence of N and P regulation across the family.

**Conclusions**

A mild reduction in N availability is sufficient to repress the P starvation response in young maize plants. The *Spx* gene family are candidates for integrating low N and low P responses.

**Key words:** maize, phosphate, nitrogen, transcriptional regulation, SPX protein family

bioRxiv preprint doi: https://doi.org/10.1101/2020.10.29.360487; this version posted October 29, 2020. The copyright holder for this preprint (which was not certified by peer review) is the author/funder, who has granted bioRxiv a license to display the preprint in perpetuity. It is made available under aCC-BY-NC-ND 4.0 International license.

## BACKGROUND

Nitrogen (N) and Phosphorus (P) are essential macronutrients required for multiple biological processes [1–5]. N is a component of chlorophyll and the proteins required for photosynthetic carbon fixation. P is required to produce the phospholipids that constitute the membranes that surround cells and intracellular organelles. N and P are both structural components of nucleic acids, including the abundant RNA molecules that play a key role in protein synthesis. The demand is such that N and P availability in agricultural soils is rarely sufficient to realize the full yield potential of crops [6, 7]. P reacts readily with other elements, such as aluminum in acid soils or calcium in alkaline soils, immobilizing it in the upper soil layers and reducing its availability to plants [8, 9]. In contrast, N, being largely present in the form of nitrate, is mobile and tends to move to deeper soil layers where it may be beyond the reach of plant root systems [10]. In low-input systems, N and P deficiencies remain a major check on production. In high-input systems, the problem is mitigated by fertilizer addition, although current levels of application are neither sustainable nor desirable given associated environmental impacts [11]. Chemical N fixation is energetically costly and contributes to greenhouse gas production [12]. High grade rock P is a non-renewable resource, predicted to be exhausted before the end of this century [13]. For these reasons, increasing N and P efficiency has been identified as a major target for plant breeding and agricultural management [11, 14].

Studies under controlled conditions have identified physiological and developmental responses to low N or low P stress, coupled with underlying large-scale changes in gene expression (the N starvation response or NSR, and P starvation response or PSR, respectively). A common response to nutrient deficiency is to increase the abundance of high-affinity transporters in roots to enhance uptake activity. Under low N, genes encoding the NTR2 nitrate transporters

bioRxiv preprint doi: https://doi.org/10.1101/2020.10.29.360487; this version posted October 29, 2020. The copyright holder for this preprint (which was not certified by peer review) is the author/funder, who has granted bioRxiv a license to display the preprint in perpetuity. It is made available under aCC-BY-NC-ND 4.0 International license.

(working on N concentrations < 250 μM) are induced [15–17]. Similarly, genes encoding PHT1 P transporters (working on P concentration < 10 μM) are induced under low P [18–21]. Further aspects of the NSR include the down-regulation of genes associated with nitrate assimilation, and amino acid, oligosaccharide and nucleic acid biosynthesis [22, 23]. The PSR includes the induction of purple acid phosphatases (PAPs) involved in recycling internal and external P from organic pools, altered polysaccharide metabolism, and remodeling of lipid membranes to reduce the requirement for phospholipids [24–26]. Interestingly, aspects of the N and P responses appear to be antagonistic [23, 25, 27, 28]. Under low N, many genes induced as part of the PSR are repressed, and *vice versa*. While molecular studies have typically addressed one nutrient deficiency at a time, it has long been appreciated that a deficiency in one element can impact the response to a second element, and that the effects of different nutrient deficiencies are not necessarily additive [29–32]. It is difficult to predict the transcriptomic response to a combination of low N and low P conditions from the single stress data – especially in the context of antagonistically regulated genes. Several studies, however, have now demonstrated clear points of molecular interaction between N and P signaling pathways.

One of the first molecular links between N and P signaling was the identification of the SPX_RING protein NITROGEN LIMITATION ADAPTATION (NLA1) in *Arabidopsis*. *Atnla* mutants fail to adapt to low nitrogen conditions and exhibit an early senescence phenotype [33] associated with Pi toxicity [34]. Further studies have shown that AtNLA directly degrades PHT1 transporters in a nitrogen-dependent manner [35] as well as the NRT1.7 nitrate transporter [36]. Under low P, down-regulation of *AtNLA* by the low P-inducible microRNA miR827 [34], promoting accumulation of PHT1. Rice OsNLA1 also regulates PHT1 abundance [37] and modulates P accumulation in a nitrogen-dependent manner [38]. However, miR827 does not

bioRxiv preprint doi: https://doi.org/10.1101/2020.10.29.360487; this version posted October 29, 2020. The copyright holder for this preprint (which was not certified by peer review) is the author/funder, who has granted bioRxiv a license to display the preprint in perpetuity. It is made available under aCC-BY-NC-ND 4.0 International license.

target *OsNla1*, nor do N and P levels regulate *OsNLA* transcript accumulation, revealing regulatory differences compared to *Arabidopsis* [37, 39].

The MYB-CC transcription factor AtPHR1 plays a central role in activating the PSR [40]. Under high P, OsPHR2, the rice ortholog of AtPHR1, is sequestered by the SPX protein OsSPX4 preventing its translocation into the nucleus and activation of PSR genes [41]. Under low P, the 26S proteasome degrades OsSPX4, allowing OsPHR2 to activate its targets. Recently, with the N-regulated OsNRT1.1b nitrate transporter has been shown to be required for OsSPX4 degradation. Under low N, levels of OsNRT1.1b are reduced, freeing OsSPX4 from turnover and leading to inhibition of the PSR [42]. Interestingly, OsSPX4 not only sequesters OsPHR2, but also the NIN-like protein OsNLP3, a central regulator of nitrogen response in rice [42]. These studies, and others, have demonstrated interaction of N and P responses, and identified the SPX proteins as important sites of coordination.

Maize is one of the world's most economically important crops. In the field, maize faces a range of abiotic stresses that affect productivity, resulting in economic losses and affecting food security. Limitation of N or P is one of the most significant checks on maize productivity worldwide [43–46]. Work in *Arabidopsis* and rice has begun to define interaction between N and P signaling networks. Nevertheless, much remains to be discovered before we can apply this knowledge to the design of more efficient management practices or the development of more nutrient efficient crop varieties. Here, we report whole transcriptome responses in the leaves and roots of maize seedlings to low N, low P and a combined low NP stress. We observed antagonism between the single low N and low P treatments, with the low N response dominating in the combined low NP treatment. We further show that even a mild reduction in N availability is sufficient to suppress the maize PSR.

bioRxiv preprint doi: https://doi.org/10.1101/2020.10.29.360487; this version posted October 29, 2020. The copyright holder for this preprint (which was not certified by peer review) is the author/funder, who has granted bioRxiv a license to display the preprint in perpetuity. It is made available under aCC-BY-NC-ND 4.0 International license.

## RESULTS

### The transcriptional response to low P is repressed under low N

To evaluate transcriptional responses to N and P limitation, we characterized leaves and roots of maize plants grown under complete nutrient conditions, under low N (9% of complete concentration), under low P (3% of complete concentration), and under combined low NP. For transcriptome analysis, plants were harvested at 25 days after emergence (DAE), when growth was first seen to be significantly reduced in the low nutrient treatments (measured as leaf surface area; Fig. S1). We grew an additional batch of plants and continued growth until 41 DAE (the limit of our PVC tube growth system) and saw that the low N treatment was more severe than the low P treatment in terms of growth reduction. Leaf surface area was indistinguishable between low N and low NP conditions at 40 DAE.

We performed RNA sequencing on the roots and shoots of 25 DAE plants and identified sets of up- and down- regulated genes (with respect to full nutrients) for each of the three stress treatments and each of the two tissues. A set of 1,555 genes were identified to be regulated in at least one comparison (leaf/root stress treatment vs control; Table S4). Of those, a similar number of genes were up-regulated as were down-regulated; a greater number of regulated genes were detected in leaves than roots. We compared the transcriptional response to the treatments by tissue and sign of the effect (up or down). There was little overlap between the response to low N and low P single stress treatments (Fig. 1A-D). When presented with the combined low NP treatment, plants broadly followed the low N response pattern: the majority of regulated genes were shared between low N and low NP; very few genes that were regulated under low P showed

bioRxiv preprint doi: https://doi.org/10.1101/2020.10.29.360487; this version posted October 29, 2020. The copyright holder for this preprint (which was not certified by peer review) is the author/funder, who has granted bioRxiv a license to display the preprint in perpetuity. It is made available under aCC-BY-NC-ND 4.0 International license.

similar regulation under low NP (Fig. 1A-D). This trend was evident in both leaves and roots, and among both up- and down- regulated genes.

We fitted a model to identify N x P interaction in the transcriptome data. Although our power to detect higher order effects was no doubt limited by the level of replication, we were able to identify 81 genes regulated by the availability of one nutrient in a manner conditional on the availability of the second (Table S4). We explored the distribution of these 81 genes across the sets of up- and down- regulated genes from the different treatments and tissues (Fig. 1E). The majority of the N x P genes were up-regulated in the low P single treatment, in either leaves, roots or both. The largest intersection was a group of 24 genes up-regulated by low P in leaves and roots, but not in any other condition, indicating this response to be lost in combined low NP stress (Fig. 1E). Many of the other low P up-regulated N x P genes were actively repressed in either low N or low NP treatments (Fig. 1E). These observations indicated that the responses to low P and low N were not only distinct, but antagonistic, and that under low NP the pattern seen under low N dominated. Of 444 genes up-regulated in leaves under low P, only 30 were up-regulated under low N, while 178 were down-regulated (Fig. 2A; Table S4). Similarly, of these 444, only 69 were up-regulated under combined low NP, with 121 down-regulated (Fig. 2A, Table S4).

To gain insight into the functional consequences of the transcriptional responses, we examined the "classical genes" (a curated set of ~5,000 well-annotated genes, many linked with existing functional data: maizegdb.org/gene_center/gene) in our regulated gene set. We supplemented the classical set with a number of additional annotations [47, 48] based on identification of maize orthologs of high-interest candidate genes previously identified in *Arabidopsis* or rice. The behavior of the top thirty (based on false discovery rate) regulated

bioRxiv preprint doi: https://doi.org/10.1101/2020.10.29.360487; this version posted October 29, 2020. The copyright holder for this preprint (which was not certified by peer review) is the author/funder, who has granted bioRxiv a license to display the preprint in perpetuity. It is made available under aCC-BY-NC-ND 4.0 International license.

classical genes mirrored the global trend - namely, strong induction under low P that was absent, or shifted to repression, in low N or low NP (Fig. 2B). Many of the top classical genes encoded functions previously associated with the PSR [49], including purple acid phosphatases (PAPs), lipid-remodeling enzymes and members of the SPX family (Fig. 2B). We further examined functional patterns using Gene Ontology (GO) analysis of the complete regulated gene set (Fig. 3C, D; Table S5). As for the single gene analysis, we observed an enrichment of terms associated with the PSR among the low P up-regulated genes that was absent in low N or low NP. This pattern extended from the general *response to P starvation* term to specific processes such as *galactolipid synthesis* (involved in lipid-remodeling under low P) and synthesis of the hormones auxin and jasmonic acid (Fig. 3C, D).

**Mild N stress is sufficient to repress the low P response**

Although low N and low P treatments were adjusted to 9 and 3% of the recommended full concentration, respectively, it was evident by 41 DAE that the low N treatment produced a greater limitation on growth than low P. As such, we speculated that the dominance of the low N transcriptional response under the combined NP treatment was simply a consequence of the greater severity of the low N stress. To address this hypothesis, we evaluated an additional set of plants under high and low P (P5 and P1, respectively; our original two P levels) in combination with five different levels of N (N5 to N1, high to low; the extremes corresponding to our previous full nutrient and low N treatments). At harvest (25 DAE), we measured shoot fresh weight (Fig. 3A-B) and again saw that the single stress combination N1P5 reduced growth more than the complementary N5P1 treatment (Fig. 3B). At intermediate N availability, however, we could observe different combinations of N and P with equivalent growth: *e.g.* N4P5 was

bioRxiv preprint doi: https://doi.org/10.1101/2020.10.29.360487; this version posted October 29, 2020. The copyright holder for this preprint (which was not certified by peer review) is the author/funder, who has granted bioRxiv a license to display the preprint in perpetuity. It is made available under aCC-BY-NC-ND 4.0 International license.

indistinguishable from N5P1 in terms of shoot fresh weight. To evaluate the impact of N availability on the PSR, we used real-time PCR to quantify the expression of a panel of selected genes. The PSR genes *Pht1;9*, *Pht1:13* (root [21]), *Mfs2* (leaf), and *Pap10* (root and leaf [50]) were strongly induced by low P under high N conditions (Fig. 3C-D). However, once N availability dropped to N4 or below, the low P induction of PSR genes was reduced or lost. Interestingly *Mfs2* and *Pap10* showed a level of expression in leaves under high P conditions that was also reduced by N limitation. Given that shoot fresh weight was the same under N5P1 and N4P1, we interpret the loss of PSR as a direct consequence of crosstalk in the N-P signaling pathways and not a secondary result of overall plant stress. We also assayed the well-characterized N responsive genes *Nir-a* and *Npf6.6* [17, 51]. As previously shown, *Nir-a* and *Npf6.6* were down-regulated by N limitation, the effect being significant at N4 and below (Fig. 3C-D, S2). Interestingly, expression of *Npf6.6* was also induced under low P in the roots, this response again being most pronounced under high N.

**P concentration in the leaves responds to both P and N availability in the substrate**

Previous studies in rice and maize have reported an increase in total P concentration in the leaves of young plants grown under low N [22, 23, 38]. As such, the antagonism observed between transcriptional responses to low N and low P might be driven by a down-regulation of PSR genes in response to higher cellular P concentration. To investigate this possibility, we quantified total P concentration using inductively coupled plasma mass spectrometry (ICP-MS) in the roots and leaves of the plants in our N-dose experiment. We found that there was indeed an increase in total P concentration in both leaves and roots under low N, in either low or high P (Fig. 4A, B). Interestingly, although low P treatment reduced P concentration as would be expected, plants

bioRxiv preprint doi: https://doi.org/10.1101/2020.10.29.360487; this version posted October 29, 2020. The copyright holder for this preprint (which was not certified by peer review) is the author/funder, who has granted bioRxiv a license to display the preprint in perpetuity. It is made available under aCC-BY-NC-ND 4.0 International license.

under combined low NP achieved a higher P concentration than those under single P stress. Although plants under low NP stress were clearly smaller than those under the single P stress, the difference in P content was maintained even when adjusted for tissue weight: the fitted value for root total P content (estimated as concentration x fresh weight) was greater for low P than high P at levels of N below N3 (Fig. 4C, D). Expressing total plant P content per unit weight of root (Fig. 4E), we again saw an indication of increased P uptake in low P plants when N was also low. Furthermore, we returned to our first experiment and quantified P concentrations in the leaves of plants grown for 41 days under the extreme N and P treatments. In these older plants, there was a clear increase in leaf P concentration under low N, most notably in high P conditions (Fig. 4F, G). Nonetheless, although we observed evidence in both 25 and 41 day-old plants of increasing P uptake under low N, P levels under combined low NP stress did not approach those seen in sufficient P conditions, indicating that P hyper-accumulation was not driving repression of the PSR under low N.

**Transcripts of the maize *Spx* gene family respond to both N and P availability**

Many studies have pointed out the importance of the SPX protein family in P homeostasis. The recent report in rice of N-dependent turnover of SPX4, a negative regulator of the PSR, suggests a mechanistic explanation for the patterns we observed in the transcriptome data. Although well described in *Arabidopsis* and rice [52], the SPX family has not been fully annotated in maize, although the SPX-EXS class has previously been described (Salazar-Vidal et al., 2016), and a number of SPX-domain genes were identified in our classical gene candidate list. To explore the role of SPX proteins in maize N and P signaling, we first identified the complete gene set from the maize genome (B73 v3.31), naming and assigning them to classes by alignment of putative

bioRxiv preprint doi: https://doi.org/10.1101/2020.10.29.360487; this version posted October 29, 2020. The copyright holder for this preprint (which was not certified by peer review) is the author/funder, who has granted bioRxiv a license to display the preprint in perpetuity. It is made available under aCC-BY-NC-ND 4.0 International license.

protein products with *Arabidopsis* and rice sequence and phylogenetic analysis (Fig. 5A, table S3). We saw broad regulation across the family in response to N and P treatments (Fig. 5B). There are four classes of SPX proteins: exclusively the SPX domain, SPX-EXS, SPX- MFS and SPX-RING domains (Secco et al. 2012). With the exception of *Spx4* in leaves, all genes in the *SPX* class were up-regulated under low P and down-regulated under low N or low NP (Fig. 5B). Similarly, the *SPX-EXS* genes *Pho1;1*, *Pho1;2b* and *Pho1;3* were up-regulated in low P and down-regulated under low N or NP. Interesting the *SPX-MFS* genes showed contrasting behaviors: *Spx-Mfs2* was up-regulated under low P and down-regulated under low N and low NP, while *Mfs1a* and *Mfs1b* were down-regulated under low P but up-regulated under low N and low NP (Fig. 5B). In rice, miR827 has shifted target preference with respect to *Arabidopsis*, from the class 4 SPX gene *Nla1* to the class 3 *Mfs* genes [39]. Similar to rice, we found miR827 target sites in the 5´UTR of *Mfs1a*, *Mfs1b* and *Mfs2*, while no site was found in the maize *Nla2* and *Mfs3* (Fig. 5, S4).

## DISCUSSION

To explore the interaction between N and P signaling pathways in maize, we characterized transcriptional responses in roots and leaves to low N, low P and combined low NP stress. We observed low N and low P responses to be distinct and antagonistic. Furthermore, under combined low NP, the low N pattern dominated, such that the classic PSR was absent, even though plant growth was P limited (as determined by comparison to plants grown under the single low N stress). Although there were differences at the level of individual genes, our low N and low P single stress results are in broad agreement with a previous report in which a similar

bioRxiv preprint doi: https://doi.org/10.1101/2020.10.29.360487; this version posted October 29, 2020. The copyright holder for this preprint (which was not certified by peer review) is the author/funder, who has granted bioRxiv a license to display the preprint in perpetuity. It is made available under aCC-BY-NC-ND 4.0 International license.

antagonism was observed, and many classic PSR genes were seen to be down-regulated under low N [23]. The rationale, or potential adaptive value, of such antagonism is not clear.

N is typically found deeper in the soil than P, reflecting differences in mobility. As a consequence, a root system optimized to access P in the topsoil will be less suited to N acquisition than a deeper root system, and *vice versa* [53–55]. In addition to occupancy of the soil column, the optimal pattern of root branching and root length is different for acquisition of N or P [53–55]. In this context, the contrasting patterns of regulation of phytohormone biosynthetic and signaling genes observed in our low N and low P root transcriptomes may mirror the differing demands placed on root system architecture.

Once acquired, P use within the plant can be maximized by continual remobilization to the point it is most needed over the growing season [3, 4]. PAPs remobilize P by releasing inorganic P from organic compounds. Induction of PAP encoding genes and increased PAP activity is a classic component of the PSR, reported in, among other organisms, *Arabidopsis* [56, 57], rice [58] and maize [50]. We observed several *Pap* genes to be up-regulated under low P in both roots and leaves. In addition to internal P remobilization, PAPs are also secreted to the rhizosphere, potentially enhancing the availability of Pi for uptake [56, 57]). The gene *Pap10* has previously been shown to be involved in scavenging external and internal Pi [59] and was one of the most clearly regulated candidates recovered from our analysis. Reflecting the global pattern, *Pap10* was strongly induced by low P, but only in full N conditions. Furthermore, constitutive expression of *Pap10* under high P was greatly reduced, even by a mild reduction in N concentration. While possible to discern antagonism in the optimization of root system architecture for N or P foraging, the benefit of suppressing P remobilization or foraging under combined low NP stress is less clear. Genes linked to lipid remodelling - the replacement of

bioRxiv preprint doi: https://doi.org/10.1101/2020.10.29.360487; this version posted October 29, 2020. The copyright holder for this preprint (which was not certified by peer review) is the author/funder, who has granted bioRxiv a license to display the preprint in perpetuity. It is made available under aCC-BY-NC-ND 4.0 International license.

membrane phospholipids by galactolipids or sulfolipids under P starvation [4, 60, 61] - followed a similar trend, the implication being that under N limitation, plants are failing to activate this well-defined aspect of the PSR. In the future, it will be informative to assay PAP activity and lipid composition under low NP.

In addition to our study, down-regulation of PSR genes under low N has been reported in at least four commercial maize hybrids and two maize inbred lines [22, 27, 62], indicating that this is a general effect not limited to specific germplasm. An isolated study that did not report such down-regulation also found no evidence of the down-regulation of N assimilation genes typically associated with N starvation, suggesting treatment and response to be acting over different time scales in this instance [63]. A similar down-regulation of PSR genes occurs in rice under prolonged N starvation [42], but not within the first 12 hours of shift to low N conditions [5], although a metabolic response can occur as early as 1 hour after such a shift [64].

Our study confirmed previous observations of P hyper-accumulation in maize leaves under N limitation [22, 23], an effect also reported in rice and *Arabidopsis* [34, 38, 65]. Initially, we considered the hypothesis that down-regulation of PSR genes in low N was a secondary response to an increase in internal total P concentration. However, low NP conditions downregulated PSR genes even when limited P availability prevented hyper-accumulation. It was intriguing to see plants under low NP accumulating P to higher concentrations than plants grown under single low P, and, indeed, reaching levels comparable to plants under full nutrients at the lowest N availability. Nonetheless, total P accumulation (adjusted for biomass) remained low in NP plants. Significantly, mild N limitation (N4) was sufficient to suppress induction of PSR genes under low P; under this same condition, P concentrations remained far below those seen at full nutrient levels, indicating that P hyper-accumulation does not drive PSR suppression.

bioRxiv preprint doi: https://doi.org/10.1101/2020.10.29.360487; this version posted October 29, 2020. The copyright holder for this preprint (which was not certified by peer review) is the author/funder, who has granted bioRxiv a license to display the preprint in perpetuity. It is made available under aCC-BY-NC-ND 4.0 International license.

Plants did perceive N reduction from N4 and below, as demonstrated by the reduced accumulation of transcripts encoding nitrate reductase (*Nir-a*), a well characterized response to N availability and changing plant N status [66]. Overall, our data support an N-mediated impact on PSR via modified signaling, rather than as the secondary effects of P hyper-accumulation. Most tellingly, young plants in our N5P1 and N4P1 treatments showed equivalent growth and P accumulation, but different patterns transcript accumulation, the latter showing almost no accumulation of the classic PSR transcripts *Pht1;9* and *Pht1;13* [21] even though P limited.

Currently, it is difficult to reconcile PSR repression and P hyper-accumulation. Under full nutrient conditions, signaling mediated by the mobile microRNA miR399 maintains the balance between P concentration in the leaves and P uptake by the roots [67, 68]. As P becomes limiting in the shoots, miR399 is produced and travels to the roots to target the *PHOSPHATE2 (PHO2) E2* ubiquitin conjugase, resulting in increased accumulation of PHT1 transporters [69–71]. Previous reports of the impact of low N on miR399 expression in maize show conflicting results, although both the nature of the low N treatment and the length of exposure have also differed [72, 73]. Although we did not see up-regulation of *Pht1* transcripts under low N, it is possible that protein levels were increased as a result of disrupted post-translational regulation, leading to increased P accumulation. Indeed, the roots of rice plants grown under low N have been shown to be more permeable to Pi [38], suggesting a greater abundance of P transporters. PHT1 proteins are inorganic $P/H^+$ symporters [74]. NRT1.1 also functions as a symporter, transporting $H^+$ and nitrate [75]. In *Arabidopsis*, a reduction of *Nrt1.1* expression leads to acidification of the growth medium [76]. Similarly, reduced nitrate transport under low N may free up protons to drive additional P transport

bioRxiv preprint doi: https://doi.org/10.1101/2020.10.29.360487; this version posted October 29, 2020. The copyright holder for this preprint (which was not certified by peer review) is the author/funder, who has granted bioRxiv a license to display the preprint in perpetuity. It is made available under aCC-BY-NC-ND 4.0 International license.

Study of NP crosstalk in *Arabidopsis* and rice has repeatedly highlighted the importance of the SPX protein family. Although first described as regulators of P homeostasis [77], SPX, SPX-RING and SPX-MFS proteins have subsequently been linked with N signaling [34, 36, 42]. The maize genome encodes 15 *SPX* family genes, the same as in rice, grouped into the four previously reported classes (*SPX*, *SPX-EXS*, *SPX-MFS* and *SPX-RING*; [52]. Small-scale differences were seen between the topology of maize and rice phylogenies, reflecting differing patterns of gene-duplication and loss. Within the *SPX-EXS* sub-family, maize contains an additional copy of *PHO1:2*, most likely resulting from paralog retention following a maize specific whole genome duplication [78]. Maize also carries additional copies of *MFS1* and *MFS3*. We did not identify a maize ortholog of *NLA1* [33], although an *NLA2* sequence was present.

N and P availability regulated transcript levels across the SPX family, consistent with a role in the integration of N and P signaling pathways. Transcripts encoding members of the single domain *Spx* class responded positively to low P in both roots and leaves, in a manner similar to *Arabidopsis* and rice [79, 80]. In rice, over-expression of *OsSPX1* and *OsSPX6* suppresses the PSR, suggesting that they act in a negative-feedback loop. Conversely, under-expression of *OsSPX1* and *OsSPX6* leads to increased P accumulation through up-regulation of genes involved in P uptake [80, 81]. Interestingly, we saw increased P accumulation coupled with down regulation of *Spx* transcripts under low N or low NP, although we did not observe any associated transcriptional induction of P uptake genes. The rice SPX4 protein exerts a further negative control on the PSR by sequestering the MYB transcription factor PHR2 in the cytosol, preventing its translocation into the nucleus and activation of target genes [41]. Under P starvation, SPX4 is degraded, freeing PHR2 to activate the PSR. It has recently

bioRxiv preprint doi: https://doi.org/10.1101/2020.10.29.360487; this version posted October 29, 2020. The copyright holder for this preprint (which was not certified by peer review) is the author/funder, who has granted bioRxiv a license to display the preprint in perpetuity. It is made available under aCC-BY-NC-ND 4.0 International license.

been reported that SPX4 turnover in rice requires the activity of the NRT1.1b [42]. Given that the abundance of NRT1.1b itself is N responsive, the NRT1-SPX4 module represents a point of integration between N and P signaling pathways. The down-regulation of *ZmNpf6.6* in leaves and roots under low N and low NP, suggesting a possible mechanism of PSR repression resulting from increased stability of SPX4.

The hyper-accumulation of P under N limitation indicates an uncoupling of P uptake from leaf P concentration [69–71]. Similar uncoupling occurs in *Arabidopsis* mutants under-expressing the SPX-EXS gene *PHO1*, in parallel with changes in subcellular partitioning of P between vacuolar stores and the cytosol [82]. The maize genome encodes two co-orthologs of the *Arabidopsis PHO1* - *Pho1;2a* and *Pho1;2b* [78]. We found both *Pho1;2a* and *Pho1;2b* to show evidence of down regulation under low N, potentially contributing to PSR repression. A further group of SPX proteins, the SPX-MFS protein family, plays a more direct role in regulating cytosolic P concentration by mediating P influx into the vacuole [83, 84]. Under low P, *OsSPX-MFS1* and *OsSPS-MFS3* are down regulated, consistent with retaining more of the total internal P pool in the cytosol for direct use [85, 86]. In contrast, *OsSPX-MFS2* is up-regulated under low P, and may be acting differently [85, 86]. The MFS2 protein, however, was not identified in a screen for vacuolar P efflux transporters [84], suggesting that it is not simply working antagonistically to MFS1 and MFS3. In maize, we found both *Mfs1* and *Mfs3* to be encoded by two genes, with both paralogs of each pair down regulated under low P in the leaves, indicating a similar function to the rice genes. *Mfs2* was found to be a single copy gene in maize, and, as in rice, to be upregulated under low P. *OsSPX-MFS1* and *OsSPX-MFS2* are targets of the low P-inducible microRNA miR827 [85, 86]. Although miR827 regulation provides a compelling link between nutrient status and SPX-MFS activity, it is hard to reconcile

bioRxiv preprint doi: https://doi.org/10.1101/2020.10.29.360487; this version posted October 29, 2020. The copyright holder for this preprint (which was not certified by peer review) is the author/funder, who has granted bioRxiv a license to display the preprint in perpetuity. It is made available under aCC-BY-NC-ND 4.0 International license.

with the contrasting patterns of regulation of *OsSPX-MFS1* and *OsSPX-MFS2*. In rice, the miR827 target site in *SPX-MFS* genes is typically located in the 5' UTR [39, 85, 86]. Interestingly, we were able to identify a putative miR827 target site in the 5'-UTR of *ZmSpx-Mfs1a, ZmSpx-Mfs1b* and *ZmSpx-Mfs2*, but not in all annotated gene models, the implication being that alternative splicing might generate miR827 resistant transcripts. Although reports are somewhat contradictory, at least one study has reported an increase in miR827 levels in maize under prolonged low N treatment [72]. In the future, it will be informative to characterize further the link between *miR827*, the SPX-MFS proteins and NP signaling.

## CONCLUSIONS

A mild reduction in nitrogen availability is sufficient to suppress the phosphate starvation response in young maize plants. Somewhat paradoxically, low nitrogen availability also results in an increase in internal phosphorus concentrations – although not to levels that might explain the repression of low phosphorus responsive genes. In cultivated fields, both nitrogen and phosphorus may be at suboptimal levels. As such, crops may grow without the classical low-phosphorus response reported in model systems, making us rethink our current understanding of low P acclimation. Further work is needed to evaluate the value of the classical phosphorus starvation response under cultivation. We might also consider the merits of biotechnological manipulation to enhance low P responses under low N conditions.

## ABBREVIATIONS

| | |
|---|---|
| DAE | Days After Emergence |
| FDR | False Discovery Rate |

bioRxiv preprint doi: https://doi.org/10.1101/2020.10.29.360487; this version posted October 29, 2020. The copyright holder for this preprint (which was not certified by peer review) is the author/funder, who has granted bioRxiv a license to display the preprint in perpetuity. It is made available under aCC-BY-NC-ND 4.0 International license.

| | |
|---|---|
| GO | Gene Ontology |
| ICP-MS | Inductively Coupled Plasma Mass Spectrometry |
| LFC | $Log_2$ Fold Change |
| NSR | Nitrogen Starvation Response |
| PCR | Polymerase Chain Reaction |
| PSR | Phosphate Starvation Response |

## DECLARATIONS

*Ethics approval and consent to participate*

Not applicable

*Consent for publication*

Not applicable

*Availability of data and materials*

Transcriptome data are available in the NCBI Sequence Read Archive under study SRP287300 at https://trace.ncbi.nlm.nih.gov/Traces/sra/?study=SRP287300

*Competing interests*

The authors declare that they have no competing interests

*Funding*

The funders had no role in study design, data collection and analysis, decision to publish, or preparation of the manuscript.

This work was supported by the Mexican Consejo Nacional de Ciencia y Tecnología (CB-2015-01 254012).

RJHS is supported by the USDA National Institute of Food and Agriculture and Hatch

bioRxiv preprint doi: https://doi.org/10.1101/2020.10.29.360487; this version posted October 29, 2020. The copyright holder for this preprint (which was not certified by peer review) is the author/funder, who has granted bioRxiv a license to display the preprint in perpetuity. It is made available under aCC-BY-NC-ND 4.0 International license.

Appropriations under Project #PEN04734 and Accession #1021929.

*Author Contributions*

JVT-R and MNS-V conceived and designed the experiments, performed the experiments, analyzed the data, prepared figures and tables and authored drafts of the paper.

RACM analyzed RNA-seq data and authored drafts of the paper.

JAM-S performed experiments, analyzed the data, and authored drafts of the paper.

CSG conceived and designed the experiments, contributed reagents/materials/analysis tools and authored or reviewed drafts of the paper.

RJHS conceived and designed the experiments, analyzed the data, contributed reagents/materials/analysis tools, prepared figures and/or tables, authored or reviewed drafts of the paper.

All authors approved the final draft.

*Acknowledgements*

We thank Benjamin Barrales-Gamez, Ana Laura Alonso-Nieves and Jessica Carcaño-Macias for assistance in plant growth and harvest.

## METHODS

*Plant material and growth conditions*

Plants in this study were maize (*Zea mays* ssp. *mays* var. W22) wild-type segregants from a larger population segregating for the *Zmpho1;2-m1.1'* mutation, generated from the stock *bti31094::Ac* (Salazar-Vidal et al., 2016). Plants were grown in the greenhouse in sand substrate with nutrient conditions maintained by a combination of fertilization with Hoagland solution [87]5mM $KNO_3$, 0.25mM $Ca(NO_3)_2$ , 2mM $MgSO_4$, 1mM $KH_2PO_4$, 20µM $FeC_6H_6O_7$, 9µM $MnSO_4$ , 1.2µM $ZnSO_4$, 0.5µM $CuSO_4$, 10µM $Na_2B_4O_7$ , 0.008µM $(NH_4)6Mo_7O_{24}$ ; [87],

bioRxiv preprint doi: https://doi.org/10.1101/2020.10.29.360487; this version posted October 29, 2020. The copyright holder for this preprint (which was not certified by peer review) is the author/funder, who has granted bioRxiv a license to display the preprint in perpetuity. It is made available under aCC-BY-NC-ND 4.0 International license.

modified as described and, where indicated, by addition of 1.5% (v/v) of P-charged acidified alumina [88]. Hoagland N concentration was adjusted by substitution of $KNO_3$ with KCl and $CaCl_2$ [89, 90]; Hoagland P concentration was adjusted by substitution of $KH_2PO_4$ with KCl. Hoagland solution was applied at 1/3 strength with the final N and P concentrations used in different experiments as stated below. For growth up to 41 days after emergence (DAE), 35 plants were evaluated in PVC tubes (15 cm diameter; 1m tall). Tubes were filled with 24 litres of washed sand. In the upper third of the tube, soil was mixed with 1.5% solid-phase P buffer (alumina-P) [88] loaded with 209 µM $KH_2PO_4$ for high P treatments and 11 µM $KH_2PO_4$ for low P treatments. Four imbibed seeds were planted at 4 cm depth per tube, thinned to a single plant a week after emergence. Plants were irrigated with distilled water up until 10 DAE after which Hoagland treatments were applied as a 1/3 strength solution, at a rate of 200 ml every third day, with final concentration: high N 1750µM $NO_3^2$; low N 157.5 $NO_3^2$; high P 333µM $KH_2PO_4$; low P 10µM $KH_2PO_4$. Plants were evaluated by non-destructive measurement of stem width, leaf number, and length of width of each fully-expanded leaf. Measurements were collected every fifth day from 10 DAE. Plants were harvested at 41 DAE. Plants were carefully removed from the tubes, minimizing damage to the root system, washed in distilled water and dried with paper towels before taking fresh weight. Tissue was dried at 42ºC for a week before taking dry weight and collecting samples for ionomic analysis (see below). For growth up to 25 DAE, 8 plants were grown in smaller PVC tubes (15 cm diameter; 50 cm tall). For RNA-seq analysis, growth conditions were identical to those used in the 41 DAE experiment, the top 30 cm of the tube including 1.5% solid-phase P buffer as in the larger tubes. Plants for RNA-seq analysis were harvested at 25 DAE, starting at 8 am. The whole plant was harvested, separating 2 cm of crown root, total root, stem and leaves. Tissue was immediately frozen in liquid nitrogen and stored at

bioRxiv preprint doi: https://doi.org/10.1101/2020.10.29.360487; this version posted October 29, 2020. The copyright holder for this preprint (which was not certified by peer review) is the author/funder, who has granted bioRxiv a license to display the preprint in perpetuity. It is made available under aCC-BY-NC-ND 4.0 International license.

-80 ºC. Samples were homogenized with cooled mortar and pistil and aliquoted under liquid nitrogen for transcriptome analysis. For the N-dose experiment, plants grown in 50 cm tubes were irrigated with combinations of P at 10 or 333 µM (P1, P5; solid-phase P buffer was not used in this experiment), and N at 157.5, 233, 350, 875 or 1750 µM (N1 to N5). Leaf and root tissue were collected at 25 DAE for gene expression and ionomic analysis.

*Determination of elemental concentration by ICP-MS analysis*

Ion concentration was determined as described previously by [91]. Briefly, root and shoot samples were analyzed by inductively coupled plasma mass spectrometry (ICP-MS) to determine the concentration of twenty metal ions. Weighed tissue samples were digested in 2.5mL concentrated nitric acid (AR Select Grade, VWR) with an added internal standard (20 ppb In, BDH Aristar Plus). Concentration of the elements B11, Na23, Mg25, Al27, P31, S34, K39, Ca43, Mn55, Fe57, Co59, Ni60, Cu65, Zn66, As75, Se82, Rb85, Sr88, Mo98 and Cd111 was measured using an Elan 6000 DRC-e mass spectrometer (Perkin-Elmer SCIEX) connected to a PFA microflow nebulizer (Elemental Scientific) and Apex HF desolvator (Elemental Scientific). A control solution was run every tenth sample to correct for machine drift both during a single run and between runs.

*RNA-sequencing analysis of differential gene expression*

RNA-sequencing analysis was carried out on roots and leaves, four NP treatments and two replicates, for a total of 2 tissues x 4 treatments x 2 replicates = 16 samples (Table S1). RNA extraction and library generation was performed by Labsergen (Laboratorio de Servicios Genomicos, Langebio, Mexico. www.langebio.cinvestav.mx/labsergen/). Libraries were prepared using the TruSeq RNA Sample Prep Kit v2

bioRxiv preprint doi: https://doi.org/10.1101/2020.10.29.360487; this version posted October 29, 2020. The copyright holder for this preprint (which was not certified by peer review) is the author/funder, who has granted bioRxiv a license to display the preprint in perpetuity. It is made available under aCC-BY-NC-ND 4.0 International license.

(https://support.illumina.com/sequencing/sequencing_kits/truseq_rna_sample_prep_kit_v2.html) and sequenced using the Illumina HiSeq4000 platform at the Vincent J. Coates Genomics Sequencing Laboratory at UC Berkeley, supported by NIH S10 OD018174 Instrumentation Grant, and at Labsergen on the Illumina NextSeq 550 equipment.

RNA sequencing reads were aligned against the AGPV3.30 maize gene model set available at Ensembl Plants [92] using kallisto version 0.43.1 [93]) (Table S1). Transcript abundance data was pre-processed using R/tximport [94] with gene-level summarization. Transcript counts were analyzed using a GLM approach in edgeR [95, 96]. We fitted the complete model *counts ~ intercept + tissue * N-level * P-level + error*. We selected genes-of-interest based on evidence of a non-zero coefficient for at least one model term containing *N-level* or *P-level* (the coef argument to R/edgeR::glmQLFTest included all model coefficients except for the intercept and *tissue* main effect; adjusted FDR < 0.01), with an absolute log fold change (LFC) > 1. Genes-of-interest were categorized based on pairwise LFC for each stress treatment with respect to the full nutrient control, LFC extracted from the model *counts ~ treatment + error*, a threshold of 1 and -1 being used for up- and down- regulation, respectively. Gene annotation was assigned as previously described in [97]. Upset diagrams were generated using R/UpSetR [98].

*Real-time PCR*

For real-time PCR transcript quantification, leaves and roots of five biological replicates per treatment were analyzed. Total RNA was extracted using Trizol and cDNAs were synthesized using SuperScript® II Reverse Transcriptase from Invitrogen (Cat No. 18064071). RT-PCR was performed using 96 well plates in a LightCycler® 480 Instrument by Roche. PCR reactions were

bioRxiv preprint doi: https://doi.org/10.1101/2020.10.29.360487; this version posted October 29, 2020. The copyright holder for this preprint (which was not certified by peer review) is the author/funder, who has granted bioRxiv a license to display the preprint in perpetuity. It is made available under aCC-BY-NC-ND 4.0 International license.

performed using KAPA SYBR FAST qPCR Master Mix kit by Kapa Biosystems, with the following cycling conditions: 95 °C for 7 min, followed by 40 cycles of 95 °C for 15 seg; 60 °C for 20 seg; 72°C for 20 seg. The final reaction volume was 10 µl including 1 µl of each 5 µM primer, 1 µl of (40 ng/µl) template cDNA, 5 µl of SYBR Master Mix and 2 µl of distilled water. The relative quantification of the gene expression was determined as $2^{\Delta Ct}$, where ΔCt = 2^(Average Ct of reference genes - Ct of gene of interest) [99]. Previously described reference genes [100] were used as controls: Cyclin-Dependent Kinase (*Cdk*; GRMZM2G149286) and a gene encoding an uncharacterized protein (*Unknown*; GRMZM2G047204). PCR primers are listed in Table S2 and were designed using Primer3Plus software [101].

*Phylogenetic analysis of the SPX family*

To find Putative SPX encoding genes and construct a phylogenetic tree, we used the methodology previously described by [50]. Briefly, *Arabidopsis* and rice proteins reported by [52] were retrieved and aligned using MUSCLE v3.8 [102]. The alignment was then converted to Stockholm format. B73 maize primary transcript predicted protein sequences v3.31 [103] obtained from Ensembl Plants [92] were searched using HMMER suite version 3.1b2 [104]. After manually checking and filtering for proteins lacking the canonical SPX domain [105], 15 putative SPX-protein sequences were identified (Table S3). In a number of cases, gene models annotated in the v4 genome assembly were preferred. For phylogenetic analysis, *Arabidopsis*, rice and maize SPX proteins were aligned using MUSCLE [102] and passed to MEGA version X [106, 107]. We manually selected SPX sub-domains defined by [52] and corrected some mismatches in the alignment (Fig. S3). A 1000 bootstrap phylogenetic tree was constructed with Maximum Likelihood method and Le_Gascuel_2008 model [108].

bioRxiv preprint doi: https://doi.org/10.1101/2020.10.29.360487; this version posted October 29, 2020. The copyright holder for this preprint (which was not certified by peer review) is the author/funder, who has granted bioRxiv a license to display the preprint in perpetuity. It is made available under aCC-BY-NC-ND 4.0 International license.

*miR827 target site prediction*

Maize *Mfs* genomic sequence and the mature miR827 [109] sequence were retrieved from maize database [110, 111] and miRbase [110], respectively. Target sites were identified using psRNATarget [112] with the recommended V2 parameters (2017 release; [113]. Target sites were graphically localized using the gene structure display server [114][115].

## FIGURE LEGENDS

**Figure 1. Transcriptional responses to low N and low P are distinct.** A) Grouping of 1555 N/P regulated genes with respect to up-regulation in leaves under low N (n; red), low P (p; yellow) or combined low N/P (np; blue) conditions in comparison with full nutrient conditions. B - D) As A) with respect to down-regulation in leaves, up-regulation in roots and down-regulation in roots, respectively. Numbers out of diagrams represent genes not present in the condition (up/down) or tissue (leaf/root). E) Upset diagram classifying some of the 81 genes that showed significant NxP interaction. Filled circles connected by line segments indicate common set membership. Colored bars at the top of the plot show the size of each set, colored by treatment comparison (colors as A-D). Black bars on the right of the plot indicate the number of genes in a given intersection.

**Figure 2. Transcript induction under low P is repressed by low N.** A) Reaction norm plot of differential transcript accumulation (LFC, $\log_2$ fold change) for 444 genes induced by low P in the leaf with respect to full nutrient conditions (full, green) under low N (n; red), low P (p; yellow) and combined low N/P (np; blue). B) Heat map showing differential transcript accumulation (z, standardized $\log_2$ fold change) with respect to NP of the top 30 (ranked by FDR in the complete model) classic genes. C) Gene ontology (GO) term enrichment (standardized $\log_{10}$ p-value; in any condition the strongest support for a given term was selected from either up- or down- regulated gene sets; values taken from down-regulation were set as negative) in differentially expressed gene sets from roots identified under n, p and np conditions with respect to full. Top GO manually curated to remove semantic redundancy. D) as C for leaf gene sets.

bioRxiv preprint doi: https://doi.org/10.1101/2020.10.29.360487; this version posted October 29, 2020. The copyright holder for this preprint (which was not certified by peer review) is the author/funder, who has granted bioRxiv a license to display the preprint in perpetuity. It is made available under aCC-BY-NC-ND 4.0 International license.

**Figure 3. Mild N stress is sufficient to repress the low P response.** A) Representative 25-day-old maize seedlings grown across five levels of N availability (N5 to N1, high to low) and two levels of P availability (P5, high and P1, low). B) Shoot fresh weight of maize seedlings grown as A. Boxes show 1st quartile, median and 3rd quartile of 4 biological replicates. Whiskers extend to the most extreme points within 1.5x box length; outlying values beyond this range are not shown. Letters indicate groups based on HSD Tukey ($p < 0.05$). Transcript accumulation (relative abundance) determined by real-time PCR for C) leaves and D) roots of 25-day-old maize seedlings grown as A. Median at least 4 biological replicates. See main text for description of genes.

**Figure 4. P accumulation responds to P and N availability.**
A) root and B) leaf P concentration (ppm dry mass) of 25-day-old maize seedlings grown across five levels of N availability (N5 to N1, high to low) and high (green points and trace) and low (yellow points and trace) levels of P availability. Large points show treatment medians; small points show individual (4) biological replicates. Dashed lines show best fit from a multiple regression model. Asterisks represent statistical significance of model terms (p value ≤ 0.001 ***; 0.001-0.01 **; 0.01-0.05 *). N, P main effect of N and P, respectively. NP, NxP interaction term. C) root and D) shoot P content (mg) estimated as concentration x total dry mass. E) Total P per unit root calculated as total P content / root dry mass. F) leaf P concentration and G) content of 41-day-old maize plants under extreme levels of N (N5, high; N1, low) and P (green, high and yellow, low) availability. Boxes show 1st quartile, median and 3rd quartile of at least 4 biological replicates. Whiskers extend to the most extreme points within 1.5x box length; outlying values beyond this range are not shown. Letters indicate groups based on HSD Tukey ($p < 0.05$).

**Figure 5. SPX family members respond to low P and low N in maize.** A) Phylogenetic tree of SPX family protein members in maize. Likelihood tree built with *Arabidopsis*, rice and maize SPX proteins. Numbers at the nodes indicate bootstrap (1000) support as percentage. B) Heat map of maize coding-SPX genes under low nitrogen (n), low phosphorus (p), and low nitrogen and phosphorus combined (np) with respect to full nutrient conditions (z, standardized $\log_2$ fold change). Asterisks indicate genes identified as regulated in the transcriptome analysis. C) Annotated *Mfs2* splice forms. Black and grey rectangles represent exonic CDS and UTR, respectively. Red marks indicate miR827 target sites. Gene models are oriented 5´to 3, from left to right.

bioRxiv preprint doi: https://doi.org/10.1101/2020.10.29.360487; this version posted October 29, 2020. The copyright holder for this preprint (which was not certified by peer review) is the author/funder, who has granted bioRxiv a license to display the preprint in perpetuity. It is made available under aCC-BY-NC-ND 4.0 International license.

**ADDITIONAL FILE1 (PDF) containing:**

**Figure S1. Maize leaf area is reduced under N and P deficiency starting at day 25 after emergence.** A) General view of plant growth system B) Square root (sqrt) of leaf surface area of plants grown under four nutrient regimes: complete nutrient solution (NP), low N (nP), low P (Np), and low N and P (np). Leaf area was quantified every 5 days from 10 days after emergence until day 40. Boxes show 1st quartile, median and 3rd quartile. Whiskers extend to the most extreme points within 1.5x box length; outlying values beyond this range are shown as filled circles. From day 20, the nature of the nutrient solution had a significant effect on growth (ANOVA; $p < 0.01$. Indicated with an asterisk). C) Sum of squares associated with N level, P level and their interaction (N x P) in an ANOVA fitted to the sqrt leaf area data. Terms significant in the analysis ($p < 0.01$) at any given day are indicated with an asterisk. Plants grown in the subsequent RNA sequencing (RNAseq) experiment were harvested at 25 DAE (arrow in B and C).

**Figure S2. Expression of selected genes across five N levels in two P levels.** Relative expression of phosphorus starvation response genes (*Pap10*, *Pht1;9*, *Pht1;13*, *Mfs2*) and nitrogen responsive genes (*Nir-a* and *Npf6.6*) in leaves and roots of 25 DAE maize plants grown in different nitrogen levels (from N1 to N5, from low to high concentration) and two phosphorus levels (P1, low; and P5, high). Colours are based on transcript abundance of each gene. Letters represent different Tukey groups by day ($p < 0.05$) based on 4 biological replicates.

**Figure S3. SPX Sub-domains used to build the phylogenetic tree.** Three sub-domain defined by [52]) were manually selected in all protein sequences used. Proteins were aligned with MUSCLE v3.8 (https://www.drive5.com/muscle/; [102].

**Figure S4. Annotated splicing variants of *Mfs1a* and *Mfs1b* have a miR827 target site in the 5´UTR.** Annotated *Mfs2* splice forms. Black and grey rectangles represent exonic CDS and UTR, respectively. Red marks indicate miR827 target sites. Gene models are oriented 5´to 3, from left to right.

**Table S1. Kallisto pseudo-alignment statistics.**

**Table S2. Genes quantified by real-time PCR under low N, low NP and low P**

**Table S3. Putative SPX-protein sequences found in maize genome V3.31.**

**Additional File 2 (XLS)**

**Table S4. 1555 genes affected at least one stress in one tissue; 81 genes that showed**

bioRxiv preprint doi: https://doi.org/10.1101/2020.10.29.360487; this version posted October 29, 2020. The copyright holder for this preprint (which was not certified by peer review) is the author/funder, who has granted bioRxiv a license to display the preprint in perpetuity. It is made available under aCC-BY-NC-ND 4.0 International license.

**significant NxP interaction; Classic genes in Figure 2; Spx genes in roots and leaves.**

**Additional File 3 (XLS)**

**Table S5. Significant ($p < 0.05$) gene ontology terms found in up- and down-regulated genes for leaves and roots in low P, low N and low NP**

bioRxiv preprint doi: https://doi.org/10.1101/2020.10.29.360487; this version posted October 29, 2020. The copyright holder for this preprint (which was not certified by peer review) is the author/funder, who has granted bioRxiv a license to display the preprint in perpetuity. It is made available under aCC-BY-NC-ND 4.0 International license.

## References

1. Ho C-H, Lin S-H, Hu H-C, Tsay Y-F. CHL1 functions as a nitrate sensor in plants. Cell. 2009;138:1184–94.

2. Plaxton WC, Tran HT. Metabolic adaptations of phosphate-starved plants. Plant Physiol. 2011;156:1006–15.

3. Péret B, Clément M, Nussaume L, Desnos T. Root developmental adaptation to phosphate starvation: better safe than sorry. Trends Plant Sci. 2011;16:442–50.

4. Veneklaas EJ, Lambers H, Bragg J, Finnegan PM, Lovelock CE, Plaxton WC, et al. Opportunities for improving phosphorus-use efficiency in crop plants. New Phytol. 2012;195:306–20.

5. Yang W, Yoon J, Choi H, Fan Y, Chen R, An G. Transcriptome analysis of nitrogen-starvation-responsive genes in rice. BMC Plant Biol. 2015;15:31.

6. Raghothama KG. PHOSPHATE ACQUISITION. Annu Rev Plant Physiol Plant Mol Biol. 1999;50:665–93.

7. Good AG, Shrawat AK, Muench DG. Can less yield more? Is reducing nutrient input into the environment compatible with maintaining crop production? Trends Plant Sci. 2004;9:597–605.

8. Hinsinger P. Bioavailability of soil inorganic P in the rhizosphere as affected by root-induced chemical changes: a review. Plant Soil. 2001;237:173–95.

9. López-Arredondo DL, Leyva-González MA, González-Morales SI, López-Bucio J, Herrera-Estrella L. Phosphate nutrition: improving low-phosphate tolerance in crops. Annu Rev Plant Biol. 2014;65:95–123.

10. Saengwilai P, Tian X, Lynch JP. Low crown root number enhances nitrogen acquisition from low-nitrogen soils in maize. Plant Physiol. 2014;166:581–9.

11. Lynch JP. Root phenotypes for improved nutrient capture: an underexploited opportunity for global agriculture. New Phytol. 2019;223:548–64.

12. Lv C, Yan C, Chen G, Ding Y, Sun J, Zhou Y, et al. An Amorphous Noble-Metal-Free Electrocatalyst that Enables Nitrogen Fixation under Ambient Conditions. Angewandte Chemie. 2018;130:6181–4. doi:10.1002/ange.201801538.

13. Vance CP, Uhde-Stone C, Allan DL. Phosphorus acquisition and use: critical adaptations by plants for securing a nonrenewable resource. New Phytol. 2003;157:423–47.

14. Herrera-Estrella L, López-Arredondo D. Phosphorus: The Underrated Element for Feeding the World. Trends Plant Sci. 2016;21:461–3.

15. Feng H, Yan M, Fan X, Li B, Shen Q, Miller AJ, et al. Spatial expression and regulation of

bioRxiv preprint doi: https://doi.org/10.1101/2020.10.29.360487; this version posted October 29, 2020. The copyright holder for this preprint (which was not certified by peer review) is the author/funder, who has granted bioRxiv a license to display the preprint in perpetuity. It is made available under aCC-BY-NC-ND 4.0 International license.

rice high-affinity nitrate transporters by nitrogen and carbon status. J Exp Bot. 2011;62:2319–32.

16. Lezhneva L, Kiba T, Feria-Bourrellier A-B, Lafouge F, Boutet-Mercey S, Zoufan P, et al. The Arabidopsis nitrate transporter NRT2.5 plays a role in nitrate acquisition and remobilization in nitrogen-starved plants. The Plant Journal. 2014;80:230–41. doi:10.1111/tpj.12626.

17. Dechorgnat J, Francis KL, Dhugga KS, Rafalski JA, Tyerman SD, Kaiser BN. Tissue and nitrogen-linked expression profiles of ammonium and nitrate transporters in maize. BMC Plant Biol. 2019;19:206.

18. Mudge SR, Rae AL, Diatloff E, Smith FW. Expression analysis suggests novel roles for members of the Pht1 family of phosphate transporters in Arabidopsis. Plant J. 2002;31:341–53.

19. Paszkowski U, Kroken S, Roux C, Briggs SP. Rice phosphate transporters include an evolutionarily divergent gene specifically activated in arbuscular mycorrhizal symbiosis. Proc Natl Acad Sci U S A. 2002;99:13324–9.

20. Wang X, Wang Y, Piñeros MA, Wang Z, Wang W, Li C, et al. Phosphate transporters OsPHT1;9 and OsPHT1;10 are involved in phosphate uptake in rice. Plant Cell Environ. 2014;37:1159–70.

21. Liu F, Xu Y, Jiang H, Jiang C, Du Y, Gong C, et al. Systematic identification, evolution and expression analysis of the Zea mays PHT1 gene family reveals several new members involved in root colonization by arbuscular mycorrhizal fungi. Int J Mol Sci. 2016;17:930.

22. Schluter U, Mascher M, Colmsee C, Scholz U, Brautigam A, Fahnenstich H, et al. Maize Source Leaf Adaptation to Nitrogen Deficiency Affects Not Only Nitrogen and Carbon Metabolism But Also Control of Phosphate Homeostasis. PLANT PHYSIOLOGY. 2012;160:1384–406. doi:10.1104/pp.112.204420.

23. Schlüter U, Colmsee C, Scholz U, Bräutigam A, Weber APM, Zellerhoff N, et al. Adaptation of maize source leaf metabolism to stress related disturbances in carbon, nitrogen and phosphorus balance. BMC Genomics. 2013;14:442.

24. Wasaki J, Yonetani R, Kuroda S, Shinano T, Yazaki J, Fujii F, et al. Transcriptomic analysis of metabolic changes by phosphorus stress in rice plant roots. Plant Cell Environ. 2003;26:1515–23.

25. Secco D, Jabnoune M, Walker H, Shou H, Wu P, Poirier Y, et al. Spatio-temporal transcript profiling of rice roots and shoots in response to phosphate starvation and recovery. Plant Cell. 2013;25:4285–304.

26. Lin H-J, Gao J, Zhang Z-M, Shen Y-O, Lan H, Liu L, et al. Transcriptional responses of maize seedling root to phosphorus starvation. Mol Biol Rep. 2013;40:5359–79.

27. Jiang L, Ball G, Hodgman C, Coules A, Zhao H, Lu C. Analysis of Gene Regulatory Networks of Maize in Response to Nitrogen. Genes . 2018;9. doi:10.3390/genes9030151.

bioRxiv preprint doi: https://doi.org/10.1101/2020.10.29.360487; this version posted October 29, 2020. The copyright holder for this preprint (which was not certified by peer review) is the author/funder, who has granted bioRxiv a license to display the preprint in perpetuity. It is made available under aCC-BY-NC-ND 4.0 International license.

28. Wang X, Wang H-F, Chen Y, Sun M-M, Wang Y, Chen Y-F. The Transcription Factor NIGT1.2 Modulates Both Phosphate Uptake and Nitrate Influx during Phosphate Starvation in Arabidopsis and Maize. The Plant Cell. 2020;:tpc.00361.2020. doi:10.1105/tpc.20.00361.

29. Cakmak I, Marschner H. Mechanism of phosphorus-induced zinc deficiency in cotton. I. Zinc deficiency-enhanced uptake rate of phosphorus. Physiologia Plantarum. 1986;68:483–90. doi:10.1111/j.1399-3054.1986.tb03386.x.

30. Pilbeam DJ, Cakmak I, Marschner H, Kirkby EA. Effect of withdrawal of phosphorus on nitrate assimilation and PEP carboxylase activity in tomato. In: Fragoso MAC, Van Beusichem ML, Houwers A, editors. Optimization of Plant Nutrition: Refereed papers from the Eighth International Colloquium for the Optimization of Plant Nutrition, 31 August – 8 September 1992, Lisbon, Portugal. Dordrecht: Springer Netherlands; 1993. p. 555–61.

31. Ward JT, Lahner B, Yakubova E, Salt DE, Raghothama KG. The effect of iron on the primary root elongation of Arabidopsis during phosphate deficiency. Plant Physiol. 2008;147:1181–91.

32. Kellermeier F, Armengaud P, Seditas TJ, Danku J, Salt DE, Amtmann A. Analysis of the Root System Architecture of Arabidopsis Provides a Quantitative Readout of Crosstalk between Nutritional Signals. Plant Cell. 2014;26:1480–96.

33. Peng M, Hannam C, Gu H, Bi Y-M, Rothstein SJ. A mutation in NLA, which encodes a RING-type ubiquitin ligase, disrupts the adaptability of Arabidopsis to nitrogen limitation. Plant J. 2007;50:320–37.

34. Kant S, Peng M, Rothstein SJ. Genetic Regulation by NLA and MicroRNA827 for Maintaining Nitrate-Dependent Phosphate Homeostasis in Arabidopsis. PLoS Genet. 2011;7:e1002021.

35. Lin W-Y, Huang T-K, Chiou T-J. NITROGEN LIMITATION ADAPTATION, a Target of MicroRNA827, Mediates Degradation of Plasma Membrane–Localized Phosphate Transporters to Maintain Phosphate Homeostasis in Arabidopsis. The Plant Cell. 2013;25:4061–74. doi:10.1105/tpc.113.116012.

36. Liu W, Sun Q, Wang K, Du Q, Li W-X. Nitrogen Limitation Adaptation (NLA) is involved in source-to-sink remobilization of nitrate by mediating the degradation of NRT1.7 in Arabidopsis. New Phytol. 2017;214:734–44.

37. Yue W, Ying Y, Wang C, Zhao Y, Dong C, Whelan J, et al. OsNLA1, a RING-type ubiquitin ligase, maintains phosphate homeostasis in Oryza sativa via degradation of phosphate transporters. Plant J. 2017;90:1040–51.

38. Zhong S, Mahmood K, Bi Y-M, Rothstein SJ, Ranathunge K. Altered Expression of OsNLA1 Modulates Pi Accumulation in Rice ( L.) Plants. Front Plant Sci. 2017;8:928.

39. Lin W-Y, Lin Y-Y, Chiang S-F, Syu C, Hsieh L-C, Chiou T-J. Evolution of microRNA827 targeting in the plant kingdom. New Phytol. 2018;217:1712–25.

bioRxiv preprint doi: https://doi.org/10.1101/2020.10.29.360487; this version posted October 29, 2020. The copyright holder for this preprint (which was not certified by peer review) is the author/funder, who has granted bioRxiv a license to display the preprint in perpetuity. It is made available under aCC-BY-NC-ND 4.0 International license.

40. Rubio V, Linhares F, Solano R, Martín AC, Iglesias J, Leyva A, et al. A conserved MYB transcription factor involved in phosphate starvation signaling both in vascular plants and in unicellular algae. Genes Dev. 2001;15:2122–33.

41. Lv Q, Zhong Y, Wang Y, Wang Z, Zhang L, Shi J, et al. SPX4 Negatively Regulates Phosphate Signaling and Homeostasis through Its Interaction with PHR2 in Rice. Plant Cell. 2014;26:1586–97.

42. Hu B, Jiang Z, Wang W, Qiu Y, Zhang Z, Liu Y, et al. Nitrate–NRT1.1B–SPX4 cascade integrates nitrogen and phosphorus signalling networks in plants. Nature Plants. 2019;5:401–13. doi:10.1038/s41477-019-0384-1.

43. Mollier A, Pellerin S. Maize root system growth and development as influenced by phosphorus deficiency. J Exp Bot. 1999;50:487–97.

44. Toledo Machado A, Fernandes MS. Participatory maize breeding for low nitrogen tolerance. Euphytica. 2001;122:567–73.

45. Lynch JP, Brown KM. Root strategies for phosphorus acquisition. In: White PJ, Hammond JP, editors. The Ecophysiology of Plant-Phosphorus Interactions. Dordrecht: Springer Netherlands; 2008. p. 83–116.

46. Ajala SO, Olaniyan AB, Olayiwola MO, Job AO. Yield improvement in maize for tolerance to low soil nitrogen. Plant Breed. 2018;137:118–26.

47. Guo A-Y, Chen X, Gao G, Zhang H, Zhu Q-H, Liu X-C, et al. PlantTFDB: a comprehensive plant transcription factor database. Nucleic Acids Res. 2008;36 Database issue:D966–9.

48. Törönen P, Medlar A, Holm L. PANNZER2: a rapid functional annotation web server. Nucleic Acids Res. 2018;46:W84–8.

49. Calderón-Vázquez C, Sawers RJH, Herrera-Estrella L. Phosphate deprivation in maize: genetics and genomics. Plant Physiol. 2011;156:1067–77.

50. González-Muñoz E, Avendaño-Vázquez A-O, Montes RAC, de Folter S, Andrés-Hernández L, Abreu-Goodger C, et al. The maize (Zea mays ssp. mays var. B73) genome encodes 33 members of the purple acid phosphatase family. Front Plant Sci. 2015;6:341.

51. Trevisan S, Manoli A, Begheldo M, Nonis A, Enna M, Vaccaro S, et al. Transcriptome analysis reveals coordinated spatiotemporal regulation of hemoglobin and nitrate reductase in response to nitrate in maize roots. New Phytol. 2011;192:338–52.

52. Secco D, Wang C, Arpat BA, Wang Z, Poirier Y, Tyerman SD, et al. The emerging importance of the SPX domain-containing proteins in phosphate homeostasis. New Phytol. 2012;193:842–51.

53. Ho MD, McCannon BC, Lynch JP. Optimization modeling of plant root architecture for water and phosphorus acquisition. J Theor Biol. 2004;226:331–40.

bioRxiv preprint doi: https://doi.org/10.1101/2020.10.29.360487; this version posted October 29, 2020. The copyright holder for this preprint (which was not certified by peer review) is the author/funder, who has granted bioRxiv a license to display the preprint in perpetuity. It is made available under aCC-BY-NC-ND 4.0 International license.

54. Postma JA, Dathe A, Lynch JP. The optimal lateral root branching density for maize depends on nitrogen and phosphorus availability. Plant Physiol. 2014;166:590–602.

55. Rangarajan H, Postma JA, Lynch JP. Co-optimization of axial root phenotypes for nitrogen and phosphorus acquisition in common bean. Ann Bot. 2018;122:485–99.

56. Li D, Zhu H, Liu K, Liu X, Leggewie G, Udvardi M, et al. Purple acid phosphatases of Arabidopsis thaliana. Comparative analysis and differential regulation by phosphate deprivation. J Biol Chem. 2002;277:27772–81.

57. Hurley BA, Tran HT, Marty NJ, Park J, Snedden WA, Mullen RT, et al. The dual-targeted purple acid phosphatase isozyme AtPAP26 is essential for efficient acclimation of Arabidopsis to nutritional phosphate deprivation. Plant Physiol. 2010;153:1112–22.

58. Zhang Q, Wang C, Tian J, Li K, Shou H. Identification of rice purple acid phosphatases related to posphate starvation signalling. Plant Biol. 2011;13:7–15.

59. Lu L, Qiu W, Gao W, Tyerman SD, Shou H, Wang C. OsPAP10c, a novel secreted acid phosphatase in rice, plays an important role in the utilization of external organic phosphorus. Plant Cell Environ. 2016;39:2247–59.

60. Nakamura Y. Phosphate starvation and membrane lipid remodeling in seed plants. Prog Lipid Res. 2013;52:43–50.

61. Pant BD, Burgos A, Pant P, Cuadros-Inostroza A, Willmitzer L, Scheible W-R. The transcription factor PHR1 regulates lipid remodeling and triacylglycerol accumulation in Arabidopsis thaliana during phosphorus starvation. J Exp Bot. 2015;66:1907–18.

62. Yang XS, Wu J, Ziegler TE, Yang X, Zayed A, Rajani MS, et al. Gene expression biomarkers provide sensitive indicators of in planta nitrogen status in maize. Plant Physiol. 2011;157:1841–52.

63. Ma N, Dong L, Lü W, Lü J, Meng Q, Liu P. Transcriptome analysis of maize seedling roots in response to nitrogen-, phosphorus-, and potassium deficiency. Plant Soil. 2020;447:637–58.

64. Hsieh P-H, Kan C-C, Wu H-Y, Yang H-C, Hsieh M-H. Early molecular events associated with nitrogen deficiency in rice seedling roots. Sci Rep. 2018;8:12207.

65. Krapp A, Berthomé R, Orsel M, Mercey-Boutet S, Yu A, Castaings L, et al. Arabidopsis roots and shoots show distinct temporal adaptation pattern towards N starvation. Plant Physiol. 2011;:111.179838.

66. Swift J, Alvarez JM, Araus V, Gutiérrez RA, Coruzzi GM. Nutrient dose-responsive transcriptome changes driven by Michaelis–Menten kinetics underlie plant growth rates. Proc Natl Acad Sci U S A. 2020;117:12531–40.

67. Chiou T-J, Aung K, Lin S-I, Wu C-C, Chiang S-F, Su C-L. Regulation of phosphate homeostasis by MicroRNA in Arabidopsis. Plant Cell. 2006;18:412–21.

bioRxiv preprint doi: https://doi.org/10.1101/2020.10.29.360487; this version posted October 29, 2020. The copyright holder for this preprint (which was not certified by peer review) is the author/funder, who has granted bioRxiv a license to display the preprint in perpetuity. It is made available under aCC-BY-NC-ND 4.0 International license.

68. Pant BD, Buhtz A, Kehr J, Scheible W-R. MicroRNA399 is a long-distance signal for the regulation of plant phosphate homeostasis. Plant J. 2008;53:731–8.

69. Bari R, Datt Pant B, Stitt M, Scheible W-R. PHO2, microRNA399, and PHR1 define a phosphate-signaling pathway in plants. Plant Physiol. 2006;141:988–99.

70. Hu B, Zhu C, Li F, Tang J, Wang Y, Lin A, et al. LEAF TIP NECROSIS1 plays a pivotal role in the regulation of multiple phosphate starvation responses in rice. Plant Physiol. 2011;156:1101–15.

71. Du Q, Wang K, Zou C, Xu C, Li W-X. The PILNCR1-miR399 Regulatory Module Is Important for Low Phosphate Tolerance in Maize. Plant Physiol. 2018;177:1743–53.

72. Xu Z, Zhong S, Li X, Li W, Rothstein SJ, Zhang S, et al. Genome-wide identification of microRNAs in response to low nitrate availability in maize leaves and roots. PLoS One. 2011;6:e28009.

73. Zhao M, Tai H, Sun S, Zhang F, Xu Y, Li W-X. Cloning and characterization of maize miRNAs involved in responses to nitrogen deficiency. PLoS One. 2012;7:e29669.

74. Nussaume L, Kanno S, Javot H, Marin E, Pochon N, Ayadi A, et al. Phosphate Import in Plants: Focus on the PHT1 Transporters. Front Plant Sci. 2011;2:83.

75. Tsay Y. The herbicide sensitivity gene CHL1 of arabidopsis encodes a nitrate-inducible nitrate transporter. Cell. 1993;72:705–13. doi:10.1016/0092-8674(93)90399-b.

76. Fang XZ, Liu XX, Zhu YX, Ye JY, Jin CW. The K and NO3- interaction mediated by NITRATE TRANSPORTER 1.1 ensures better plant growth under K -limiting conditions. Plant Physiology. 2020;:01229.2020. doi:10.1104/pp.20.01229.

77. Rouached H, Bulak Arpat A, Poirier Y. Regulation of Phosphate Starvation Responses in Plants: Signaling Players and Cross-Talks. Molecular Plant. 2010;3:288–99. doi:10.1093/mp/ssp120.

78. Salazar-Vidal MN, Acosta-Segovia E, Sánchez-León N, Ahern KR, Brutnell TP, Sawers RJH. Characterization and Transposon Mutagenesis of the Maize (Zea mays) Pho1 Gene Family. PLoS One. 2016;11:e0161882.

79. Wang Z, Hu H, Huang H, Duan K, Wu Z, Wu P. Regulation of OsSPX1 and OsSPX3 on Expression ofOsSPXdomain Genes and Pi-starvation Signaling in Rice. Journal of Integrative Plant Biology. 2009;51:663–74. doi:10.1111/j.1744-7909.2009.00834.x.

80. Zhong Y, Wang Y, Guo J, Zhu X, Shi J, He Q, et al. Rice SPX6 negatively regulates the phosphate starvation response through suppression of the transcription factor PHR2. New Phytol. 2018;219:135–48.

81. Wang C, Ying S, Huang H, Li K, Wu P, Shou H. Involvement of OsSPX1 in phosphate homeostasis in rice. Plant J. 2009;57:895–904.

bioRxiv preprint doi: https://doi.org/10.1101/2020.10.29.360487; this version posted October 29, 2020. The copyright holder for this preprint (which was not certified by peer review) is the author/funder, who has granted bioRxiv a license to display the preprint in perpetuity. It is made available under aCC-BY-NC-ND 4.0 International license.

82. Rouached H, Stefanovic A, Secco D, Bulak Arpat A, Gout E, Bligny R, et al. Uncoupling phosphate deficiency from its major effects on growth and transcriptome via PHO1 expression in Arabidopsis. Plant J. 2011;65:557–70.

83. Liu T-Y, Huang T-K, Yang S-Y, Hong Y-T, Huang S-M, Wang F-N, et al. Identification of plant vacuolar transporters mediating phosphate storage. Nat Commun. 2016;7:11095.

84. Xu L, Zhao H, Wan R, Liu Y, Xu Z, Tian W, et al. Identification of vacuolar phosphate efflux transporters in land plants. Nat Plants. 2019;5:84–94.

85. Lin S-I, Santi C, Jobet E, Lacut E, El Kholti N, Karlowski WM, et al. Complex Regulation of Two Target Genes Encoding SPX-MFS Proteins by Rice miR827 in Response to Phosphate Starvation. Plant Cell Physiol. 2010;51:2119–31.

86. Wang C, Huang W, Ying Y, Li S, Secco D, Tyerman S, et al. Functional characterization of the rice SPX-MFS family reveals a key role of OsSPX-MFS1 in controlling phosphate homeostasis in leaves. New Phytol. 2012;196:139–48.

87. Hoagland DR, Broyer TC. GENERAL NATURE OF THE PROCESS OF SALT ACCUMULATION BY ROOTS WITH DESCRIPTION OF EXPERIMENTAL METHODS. Plant Physiol. 1936;11:471–507.

88. Lynch J, Epstein E, Lauchli A, Weight GI. An automated greenhouse sand culture system suitable for studies of P nutrition. Plant Cell Environ. 1990;13:547–54.

89. Zhao D, Reddy KR, Kakani VG, Reddy VR. Nitrogen deficiency effects on plant growth, leaf photosynthesis, and hyperspectral reflectance properties of sorghum. Eur J Agron. 2005;22:391–403.

90. Reddy AR, Reddy KR, Padjung R, Hodges HF. Nitrogen nutrition and photosynthesis in leaves of Pima cotton 1. J Plant Nutr. 1996;19:755–70.

91. Ramírez-Flores MR, Rellán-Álvarez R, Wozniak B, Gebreselassie M-N, Jakobsen I, Olalde-Portugal V, et al. Co-ordinated Changes in the Accumulation of Metal Ions in Maize (Zea mays ssp. mays L.) in Response to Inoculation with the Arbuscular Mycorrhizal Fungus Funneliformis mosseae. Plant Cell Physiol. 2017;58:1689–99.

92. ftp://ftp.ensemblgenomes.org/pub/plants/release-30/.

93. Bray NL, Pimentel H, Melsted P, Pachter L. Near-optimal probabilistic RNA-seq quantification. Nat Biotechnol. 2016;34:525–7.

94. Soneson C, Love MI, Robinson MD. Differential analyses for RNA-seq: transcript-level estimates improve gene-level inferences. F1000Res. 2015;4:1521.

95. Robinson MD, McCarthy DJ, Smyth GK. edgeR: a Bioconductor package for differential expression analysis of digital gene expression data. Bioinformatics. 2010;26:139–40.

bioRxiv preprint doi: https://doi.org/10.1101/2020.10.29.360487; this version posted October 29, 2020. The copyright holder for this preprint (which was not certified by peer review) is the author/funder, who has granted bioRxiv a license to display the preprint in perpetuity. It is made available under aCC-BY-NC-ND 4.0 International license.

96. McCarthy DJ, Chen Y, Smyth GK. Differential expression analysis of multifactor RNA-Seq experiments with respect to biological variation. Nucleic Acids Res. 2012;40:4288–97.

97. Gonzalez-Segovia E, Pérez-Limon S, Cíntora-Martínez GC, Guerrero-Zavala A, Janzen GM, Hufford MB, et al. Characterization of introgression from the teosinte ssp. to Mexican highland maize. PeerJ. 2019;7:e6815.

98. Conway JR, Lex A, Gehlenborg N. UpSetR: an R package for the visualization of intersecting sets and their properties. Bioinformatics. 2017;33:2938–40.

99. Massange-Sanchez JA, Palmeros-Suarez PA, Espitia-Rangel E, Rodriguez-Arevalo I, Sanchez-Segura L, Martinez-Gallardo NA, et al. Overexpression of grain amaranth (Amaranthus hypochondriacus) AhERF or AhDOF transcription factors in Arabidopsis thaliana increases water deficit-and salt-stress tolerance, respectively, via contrasting stress-amelioration mechanisms. PLoS One. 2016;11:e0164280.

100. Lin F, Jiang L, Liu Y, Lv Y, Dai H, Zhao H. Genome-wide identification of housekeeping genes in maize. Plant Mol Biol. 2014;86:543–54.

101. Untergasser A, Nijveen H, Rao X, Bisseling T, Geurts R, Leunissen JAM. Primer3Plus, an enhanced web interface to Primer3. Nucleic Acids Res. 2007;35 Web Server issue:W71–4.

102. Edgar RC. MUSCLE: multiple sequence alignment with high accuracy and high throughput. Nucleic Acids Res. 2004;32:1792–7.

103. Schnable PS, Ware D, Fulton RS, Stein JC, Wei F, Pasternak S, et al. The B73 maize genome: complexity, diversity, and dynamics. Science. 2009;326:1112–5.

104. Finn RD, Clements J, Eddy SR. HMMER web server: interactive sequence similarity searching. Nucleic Acids Research. 2011;39 suppl:W29–37. doi:10.1093/nar/gkr367.

105. www.ncbi.nlm.nih.gov/protein.

106. Kumar S, Stecher G, Li M, Knyaz C, Tamura K. MEGA X: Molecular Evolutionary Genetics Analysis across Computing Platforms. Mol Biol Evol. 2018;35:1547–9.

107. Stecher G, Tamura K, Kumar S. Molecular Evolutionary Genetics Analysis (MEGA) for macOS. Mol Biol Evol. 2020;37:1237–9.

108. Le SQ, Gascuel O. An improved general amino acid replacement matrix. Mol Biol Evol. 2008;25:1307–20.

109. Zhang L, Chia J-M, Kumari S, Stein JC, Liu Z, Narechania A, et al. A genome-wide characterization of microRNA genes in maize. PLoS Genet. 2009;5:e1000716.

110. http://www.mirbase.org/.

111. https://www.maizegdb.org/.

bioRxiv preprint doi: https://doi.org/10.1101/2020.10.29.360487; this version posted October 29, 2020. The copyright holder for this preprint (which was not certified by peer review) is the author/funder, who has granted bioRxiv a license to display the preprint in perpetuity. It is made available under aCC-BY-NC-ND 4.0 International license.

112. http://plantgrn.noble.org/psRNATarget/.

113. Dai X, Zhuang Z, Zhao PX. psRNATarget: a plant small RNA target analysis server (2017 release). Nucleic Acids Res. 2018;46:W49–54.

114. http://gsds.gao-lab.org/.

115. Hu B, Jin J, Guo A-Y, Zhang H, Luo J, Gao G. GSDS 2.0: an upgraded gene feature visualization server. Bioinformatics. 2015;31:1296–7.

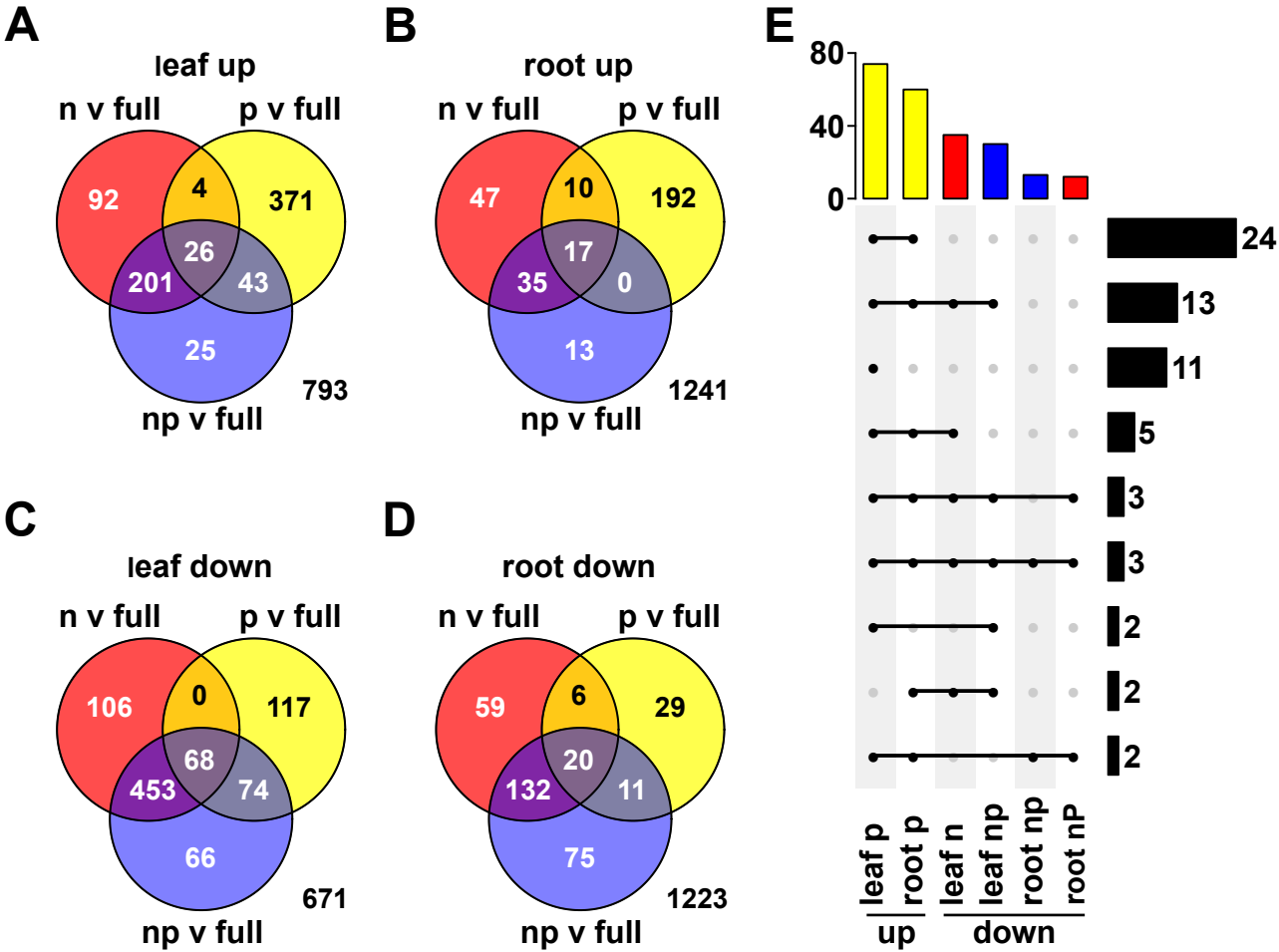
A
leaf up
n v full
p v full
np v full
92
4
371
26
201
43
25
793
B
root up
n v full
p v full
np v full
47
10
192
17
35
0
13
1241
C
leaf down
n v full
p v full
np v full
106
0
117
68
453
74
66
671
D
root down
n v full
p v full
np v full
59
6
29
20
132
11
75
1223
E
80
40
0
24
13
11
5
3
3
2
2
2
leaf p
root p
leaf n
leaf np
root np
root nP
up
down

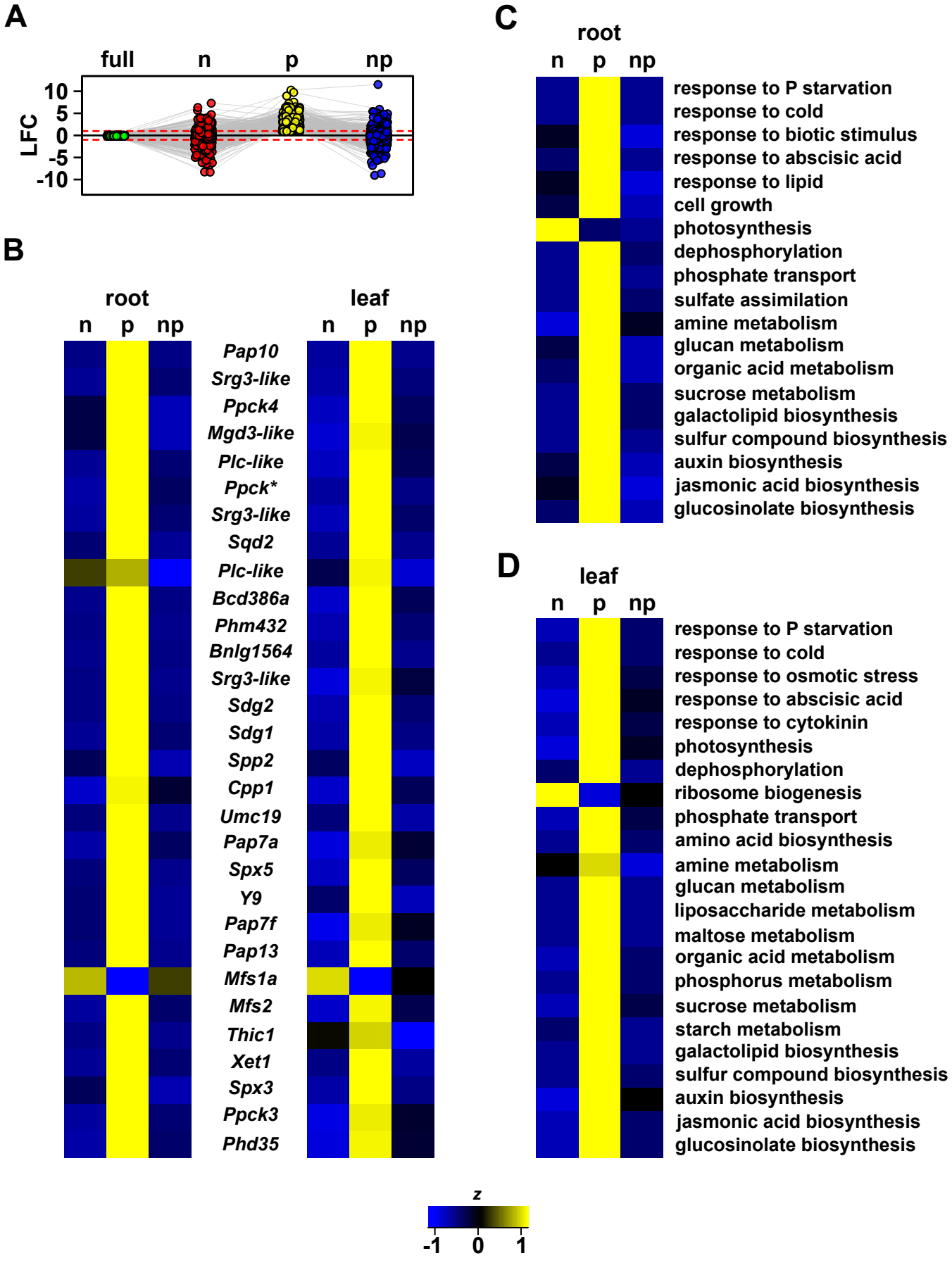
A
full
n
p
np
LFC
10
5
0
-5
-10
B
root
n p np
leaf
n p np
Pap10
Srg3-like
Ppck4
Mgd3-like
Plc-like
Ppck*
Srg3-like
Sqd2
Plc-like
Bcd386a
Phm432
Bnlg1564
Srg3-like
Sdg2
Sdg1
Spp2
Cpp1
Umc19
Pap7a
Spx5
Y9
Pap7f
Pap13
Mfs1a
Mfs2
Thic1
Xet1
Spx3
Ppck3
Phd35
C
root
n p np
response to P starvation
response to cold
response to biotic stimulus
response to abscisic acid
response to lipid
cell growth
photosynthesis
dephosphorylation
phosphate transport
sulfate assimilation
amine metabolism
glucan metabolism
organic acid metabolism
sucrose metabolism
galactolipid biosynthesis
sulfur compound biosynthesis
auxin biosynthesis
jasmonic acid biosynthesis
glucosinolate biosynthesis
D
leaf
n p np
response to P starvation
response to cold
response to osmotic stress
response to abscisic acid
response to cytokinin
photosynthesis
dephosphorylation
ribosome biogenesis
phosphate transport
amino acid biosynthesis
amine metabolism
glucan metabolism
liposaccharide metabolism
maltose metabolism
organic acid metabolism
phosphorus metabolism
sucrose metabolism
starch metabolism
galactolipid biosynthesis
sulfur compound biosynthesis
auxin biosynthesis
jasmonic acid biosynthesis
glucosinolate biosynthesis
z
-1
0
1

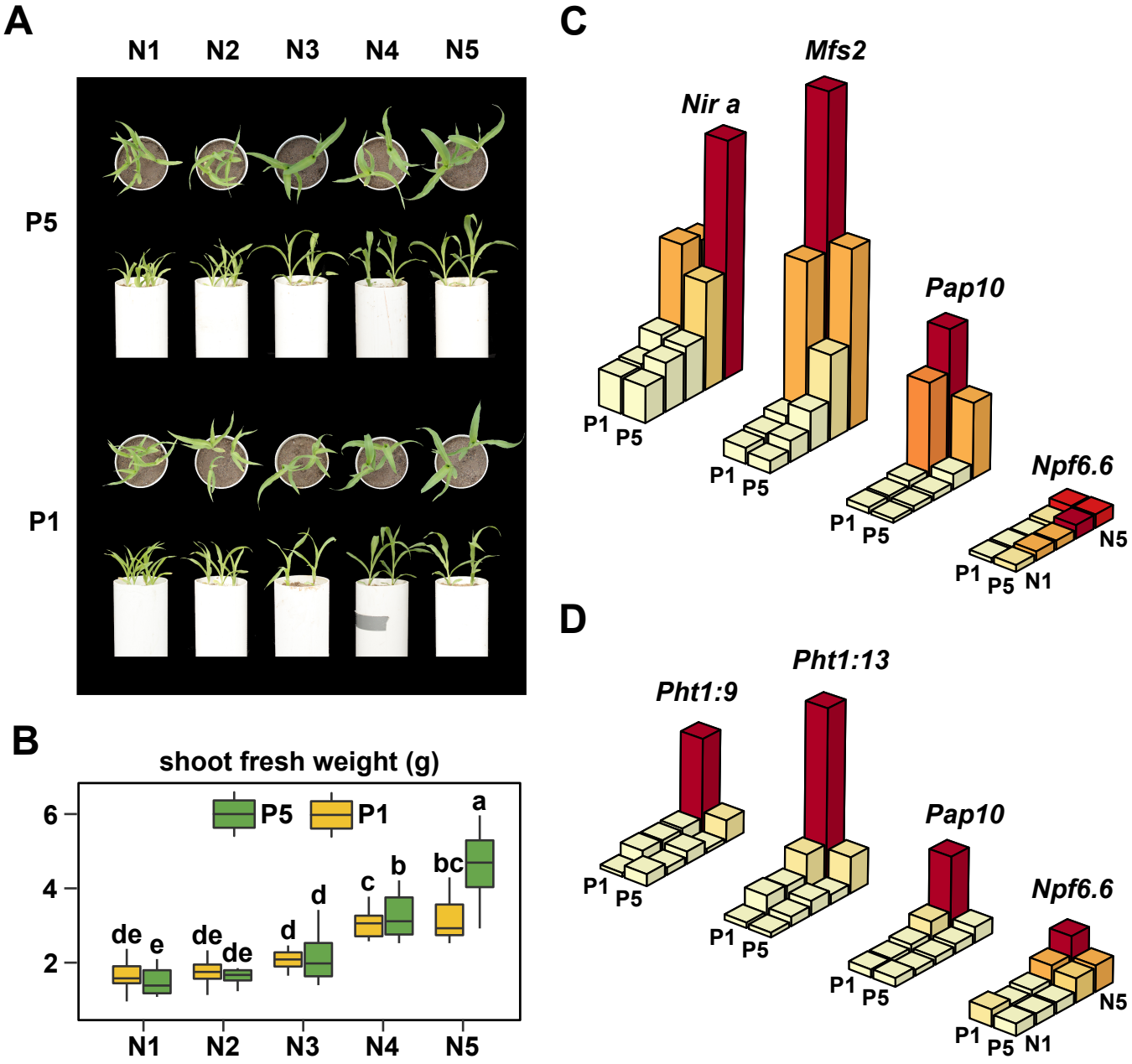
A
N1
N2
N3
N4
N5
P5
P1
B
shoot fresh weight (g)
6
4
2
P5
P1
a
bc
b
c
d
d
de
e
de
de
N1
N2
N3
N4
N5
C
Mfs2
Nir a
Pap10
Npf6.6
P1
P5
N1
N5
D
Pht1:13
Pht1:9
Pap10
Npf6.6
P1
P5
N1
N5

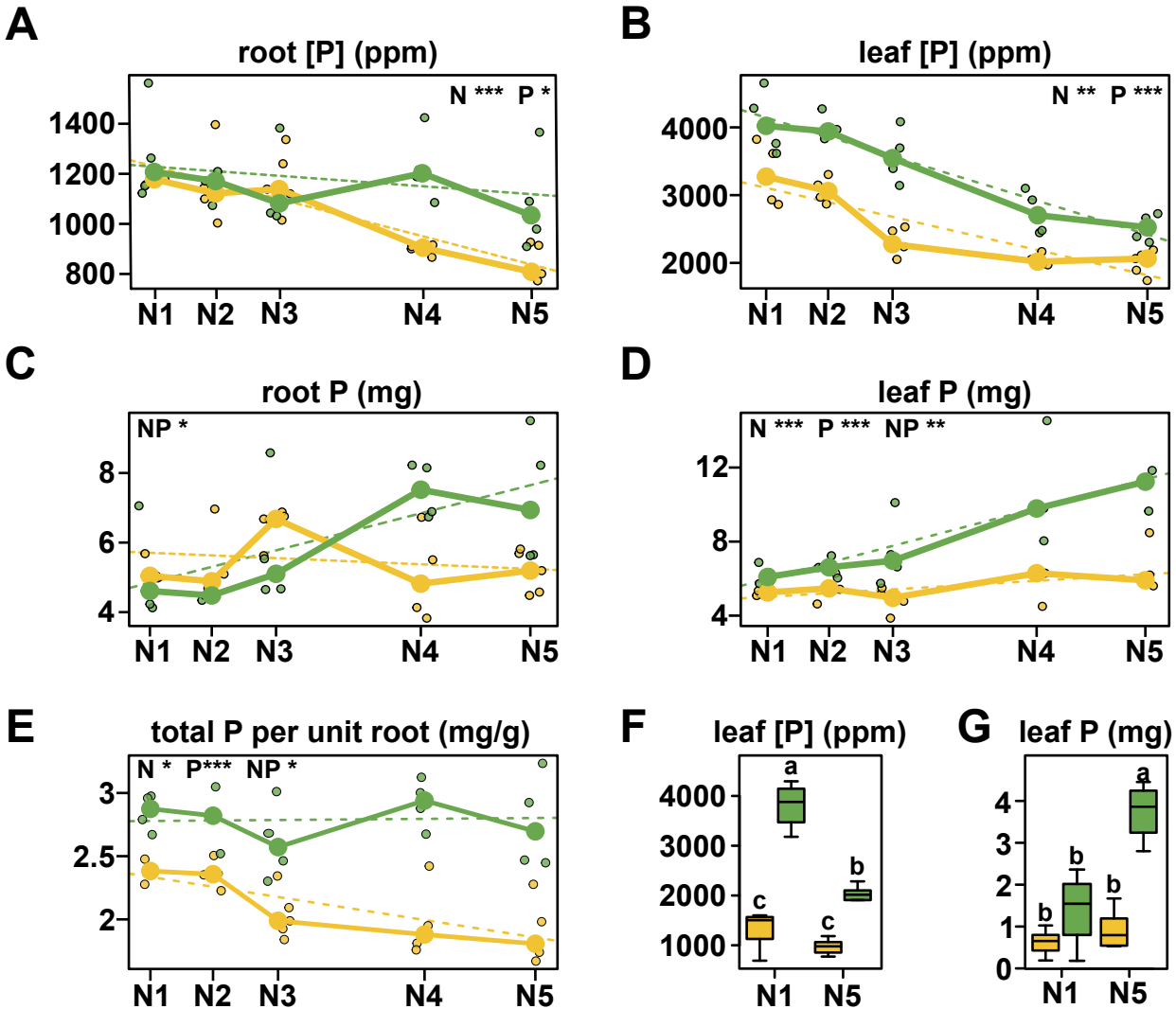
A
root [P] (ppm)
N *** P *
1400
1200
1000
800
N1 N2 N3 N4 N5
B
leaf [P] (ppm)
N ** P ***
4000
3000
2000
N1 N2 N3 N4 N5
C
root P (mg)
NP *
8
6
4
N1 N2 N3 N4 N5
D
leaf P (mg)
N *** P *** NP **
12
8
4
N1 N2 N3 N4 N5
E
total P per unit root (mg/g)
N * P*** NP *
3
2.5
2
N1 N2 N3 N4 N5
F
leaf [P] (ppm)
a
b
c
c
4000
3000
2000
1000
N1 N5
G
leaf P (mg)
a
b
b
b
4
3
2
1
0
N1 N5

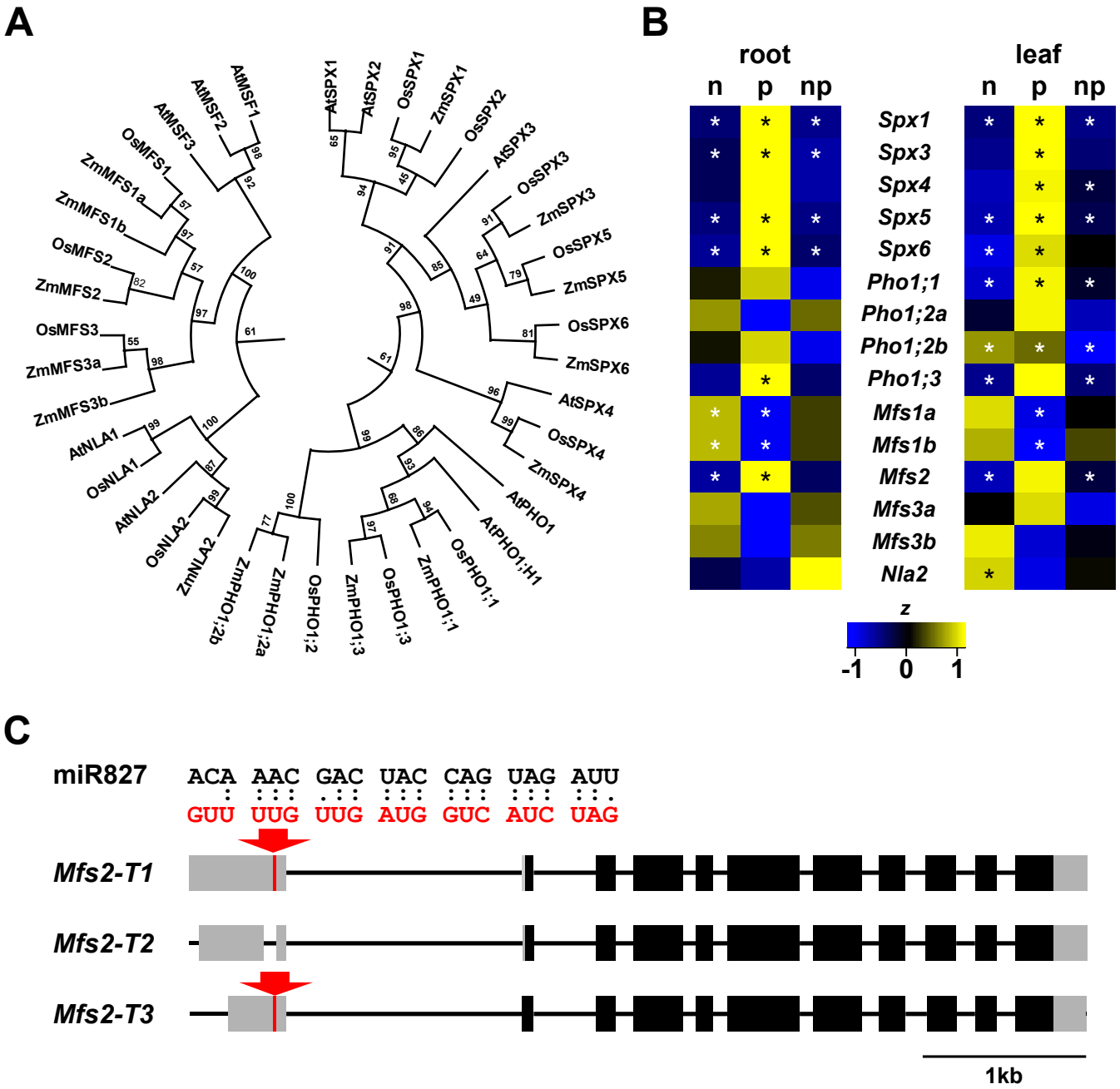
A
AtMSF1
AtMSF2
AtMSF3
OsMFS1
ZmMFS1a
ZmMFS1b
OsMFS2
ZmMFS2
OsMFS3
ZmMFS3a
ZmMFS3b
AtNLA1
OsNLA1
AtNLA2
OsNLA2
ZmNLA2
AtSPX1
AtSPX2
OsSPX1
ZmSPX1
OsSPX2
AtSPX3
OsSPX3
ZmSPX3
OsSPX5
ZmSPX5
OsSPX6
ZmSPX6
AtSPX4
OsSPX4
ZmSPX4
AtPHO1
AtPHO1;H1
OsPHO1;1
ZmPHO1;1
OsPHO1;3
ZmPHO1;3
OsPHO1;2
ZmPHO1;2a
ZmPHO1;2b
B
root
leaf
n
p
np
Spx1
Spx3
Spx4
Spx5
Spx6
Pho1;1
Pho1;2a
Pho1;2b
Pho1;3
Mfs1a
Mfs1b
Mfs2
Mfs3a
Mfs3b
Nla2
z
-1
0
1
C
miR827
ACA AAC GAC UAC CAG UAG AUU
GUU UUG UUG AUG GUC AUC UAG
Mfs2-T1
Mfs2-T2
Mfs2-T3
1kb